PRACTICAL DESIGN AGAINST TORSIONAL VIBRATION

by
Mark A. Corbo
Project Design Engineer
and
Stanley B. Malanoski
Manager, Engineering Services
Mechanical Technology Incorporated
Latham, New York

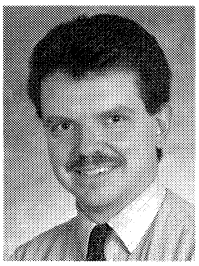

Mark A. Corbo is a Project Design Engineer with Mechanical Technology Incorporated, a high technology engineering/ consulting firm. In this position, he is responsible for performing analytical studies, troubleshooting, and design audits in the areas of rotordynamics, fluid-film lubrication, and hydraulics for various customers within the turbomachinery industry. Prior to joining MTI in 1995, he spent 12 years in the aerospace industry designing and analyzing pumps, valves, controls, and electromechanical components for gas turbine engines. His fields of expertise include rotordynamics, journal bearings, incompressible and compressible flow, computational fluid dynamics, stress analysis, finite element analysis, dynamic simulations, and mechanical design. He holds B.S. and M.S. degrees (Mechanical Engineering) from Rensselaer Polytechnic Institute. He is a member of ASME.

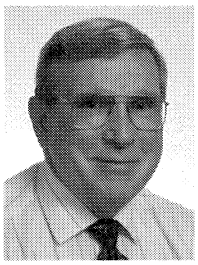

Stanley B. Malanoski is a graduate Mechanical Engineer and Manager of Engineering Services at Mechanical Technology Incorporated's Technology Division. He has over 30 years of industrial experience in the areas of turbomachinery design, analysis, and troubleshooting. Mr. Malanoski's fields of special competence are in the management of engineering personnel and programs; dynamic analysis of practical rotor-bearing systems; squeeze-film damper design, analysis and application; and fluid-film bearing/seal and system designs, including process fluid (gas and liquid) lubrication. He is author or coauthor of over 50 technical publications and hundreds of Mechanical Technology Incorporated technical reports.

ABSTRACT

One of the foremost concerns facing turbomachinery users today is that of torsional vibration. In contrast to lateral vibration problems, torsional failures are especially heinous since the first symptom of a problem is often a broken shaft, gear tooth, or coupling. The difficulty of detecting incipient failures in the field makes the performance of a thorough torsional vibration analysis an essential component of the turbomachinery design process.

The authors' purpose is to provide users with a practical design procedure that can be used to ensure that their systems will not encounter major difficulties in the field. It has been the authors' experience that most turbomachinery users encounter little difficulty in determining their machine's natural frequencies due to the large number of resources available in that area. However, problems often arise when they must translate this information into an accurate prediction of whether or not their design will experience torsional vibration problems. Accordingly, this presentation concentrates on the steps that should be taken once the natural frequencies have been found.

A cursory review is presented of popular procedures, such as Holzer's method, for obtaining the machine's natural frequencies and mode shapes. This area is purposely limited in detail since there are many excellent resources in the literature that may be consulted for a more rigorous treatment.

The generation of an interference or Campbell diagram is then treated in far more detail. Of particular interest is generation of the upward sloping lines representing the system's excitation frequencies. The various excitation sources commonly found in turbomachinery, such as gears, vaned impellers, and electric motors, are discussed along with the excitation frequencies that each introduces into the system. The unique problems associated with the startup of systems driven by synchronous motors are also described.

Once the interference points have been generated, the user then generally has two choices for dealing with them. Either design changes, such as alteration of couplings, are implemented to eliminate the interferences or the interference points are subjected to further analysis. Many users automatically opt for the first alternative, since they believe they must avoid resonance conditions at all costs. While this is an admirable and worthy goal under ideal circumstances, the cost of achieving it is often unwieldy.

Instead, the procedure provided herein advocates analysis of all interference points prior to the implementation of costly design changes. The analysis might be as simple as inspection of the appropriate mode shape or the unit's torque *vs* speed curve. Interference points can frequently be eliminated from consideration based on these inspections revealing that the induced torques are negligible. The resonant points that cannot be thereby removed should be investigated using a damped forced vibration analysis.

Detailed guidelines for performing the damped analysis are presented herein. Methods for determining the magnitudes and locations of excitation torques for various machinery classes are given. Procedures are provided for obtaining damping coefficients for typical sources such as impellers, shaft material hysteresis, and couplings. Finally, users are provided with ground rules for utilizing the calculated cyclic torques and stresses to determine their design's adequacy.

If the analysis identifies problem areas, practical and relatively simple rectification methods are provided. Lastly, a complete

step-by-step analysis procedure is given that summarizes the entire preceding discussion. This methodology can be utilized in the design of virtually any turbomachinery system the user may encounter.

INTRODUCTION

Torsional vibration is a subject that should be of concern to all turbomachinery users. The word "users," utilized throughout this work, refers to all engineers, including designers, analysts, managers, and operators, involved in the design, manufacture, and/or operation of turbomachinery. By some accounts, torsional vibration is the leading cause of failures in turbomachinery drive trains. Some typical effects of uncontrolled torsional vibration are failed couplings, broken shafts, worn gears and splines, and fractured gear teeth. Accordingly, a thorough torsional vibration analysis should be included as an integral part of the design process. A thorough analysis procedure that can be practically implemented by turbomachinery users is the primary subject here.

Although it is felt that all types of engineers who work with turbomachinery can gain a flavor for the subject from the information presented herein, the presentation is primarily directed towards mechanical engineers. Specifically, it is meant to aid those mechanical engineers responsible for the design and analysis of turbomachinery drive trains. It is the opinion of the authors that most torsional vibration problems experienced in the field can be prevented by taking prudent action during the design process.

Although many turbomachinery users are intimately familiar with the fundamentals of torsional vibration, the authors are acquainted with some who are not. For their benefit, a brief review of the basics is, thus, in order.

For illustrative purposes, any turbomachinery assembly can be approximated by two inertias or disks connected by a torsional spring as is shown in Figure 1. One inertia can be taken to represent the system's driving element, which is usually a turbine or motor while the second corresponds to the driven load such as a compressor or pump impeller. The torsional spring between them is a simplified representation for the interconnecting shafting.

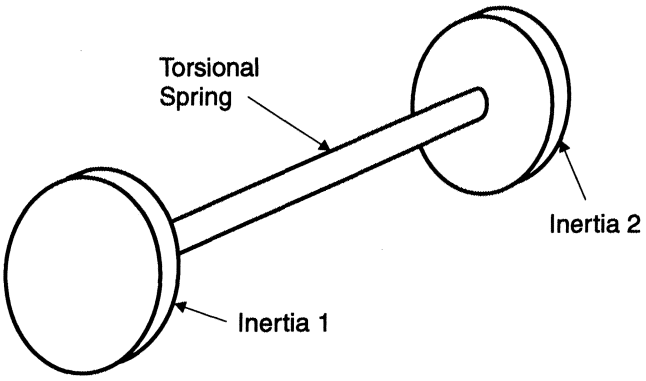

Figure 1. Two Inertia Torsional System.

When the machine is at rest, the two inertias are stationary and the shaft is unstressed in its free position. When the machine is started and brought up to steady speed, the driving and load torques become equal and the two disks rotate at the same velocity. However, the shaft is twisted away from its free position by an angle equal to the transmitted torque divided by its spring rate. This position will be referred to as the equilibrium position.

If the driver and load torques were then suddenly removed from the assembly, the twisted spring would uncoil, propelling the two disks in opposite directions with respect to the shaft. If there was no damping present, the disks would rotate to the free position and continue past until the spring was twisted by an equal amount in the opposite direction. Oscillations would continue indefinitely with the system continually exchanging the potential energy of the spring for kinetic energy in the inertias. These vibrations have no effect on the system's average speed, which remains constant.

This phenomenon is known as undamped free torsional vibration and is fully analogous to the well-known linear mass-spring system. Regardless of the initial conditions existing prior to vibration, the system always oscillates at a specific frequency, known as the undamped natural frequency. The natural frequency is a function of the disks' inertias and the shaft's stiffness and is, thus, a characteristic of the system.

Forced vibration can be illustrated with the same system by superimposing a sinusoidally varying torque on the steady torque of either of the disks. The resulting imbalance between driver and load torques would cause all elements to vibrate about the equilibrium position. Consequently, all elements would experience sinusoidal fluctuations in torque and speed about their average values.

The magnitudes of the induced cyclic torques in the second disk and connecting shaft would be dependent on the dynamic characteristics of the system. The response is controlled by the ratio of the excitation frequency to the natural frequency, as is illustrated in the well-known undamped response curve for a one degree of freedom system shown in Figure 2. The ordinate on this figure is the ratio of the induced shaft torque to the excitation torque and is referred to as the dynamic magnifier.

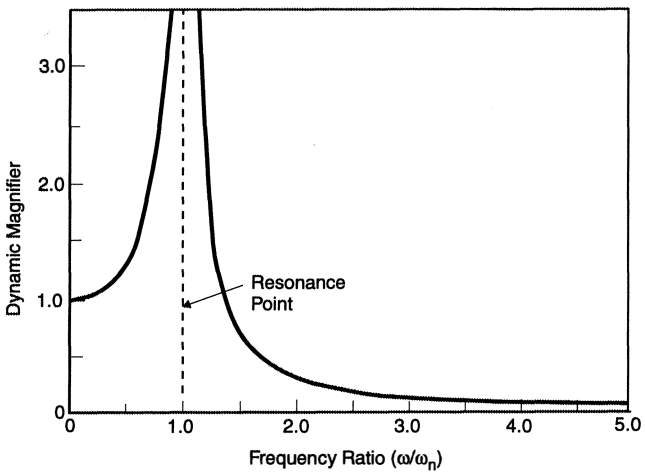

Figure 2. Undamped Response Curve for One D.O.F. System.

It is seen that when the driving frequency is equal to the system's natural frequency, the dynamic magnifier is theoretically infinite. This condition is known as resonance and represents a potential problem for the system. Although the actual response in practice is not infinite due to the presence of finite damping in all systems, huge amplifications can still occur which produce large cyclic stresses in the shaft.

These high stresses can often lead to shaft fatigue. Additionally, the large generated peak torques can overload components such as gears, splines, and couplings. Therefore, the essence of torsional vibration analysis is identification of all resonance points and determination of the system's ability to withstand them.

Comparison with Lateral Vibration

Many readers may be more familiar with lateral vibration than its torsional counterpart. Such knowledge is helpful since the two phenomena are similar in many ways. However, there are several important differences, including the following:

- In lateral vibrations, the natural frequencies are often functions of the operating speed due to their dependence on fluid-film bearing stiffness. Conversely, torsional natural frequencies are independent of operating speed.
- In lateral vibrations, large vibratory motions can cause severe problems. On the other hand, the primary parameters of concern in torsional vibration are induced torques and stresses. The actual displacements are usually of academic interest only.
- In the most common lateral mode, synchronous whirling, the shaft does not undergo stress reversals. The bending stress is essentially constant and shaft fatigue is not a concern. Conversely, torsional vibrations always induce cyclic stresses that can lead to fatigue.
- Unlike lateral vibrations, torsional vibration problems usually cannot be corrected by balancing the machine more precisely.

Topics Not Covered

Although this presentation is intended to be comprehensive, there are some subjects within the field of torsional vibration that are not addressed. The amount of information related to this topic is far too voluminous to cover in a single tutorial. The authors have, therefore, attempted to limit the covered material to areas that a practical mechanical engineer needs to know in order to perform a complete torsional analysis on a turbomachinery drive train. Accordingly, the following subjects are either partially or totally neglected in this work:

Distributed parameter models. Since most practical systems can be modelled accurately using them, the discussion is limited to lumped parameter models. The procedures utilized with a distributed parameter model are similar to those specified herein, although they are more complicated. Vance [1] points out that the main difference is that the ordinary differential equations of the lumped model are replaced by partial differential equations. Distributed parameter models are discussed to various extents by Ker Wilson [2], Eshleman [3], Bisshopp [4], and Triezenberg [5].

Coupled lateral-torsional vibrations. There are some instances, particularly in machines containing gears, where a strong coupling between lateral and torsional modes can arise. The procedure required to analyze such a phenomenon would require an entire paper of its own. Additionally, Simmons and Smalley [6] claim that the presence of lateral vibration has very little impact on the torsional natural frequencies and mode shapes. Thus, with the exception of the effect it can have on journal bearing damping, this phenomenon is not addressed. Lund [7] provides a description of this topic for the interested reader.

Reciprocating machines. In order to maintain this work at a manageable length, its scope is limited to rotary machines. The classic texts by Ker Wilson [2] and Nestorides [8] are among the large number of works that describe the excitations generated in reciprocating engines and methods for converting their reciprocating masses into equivalent rotary inertias.

Torsional vibration dampers. Although the damping introduced by common turbomachinery components is discussed in great detail, devices that are used for the sole purpose of introducing damping into the assembly are not addressed. These devices, which include Lanchester dampers, specialized oil-filled couplings, and Holset couplings, are described by O'Connor [9], Den Hartog and Ormondroyd [10], and Brown [11].

Electrical-mechanical analogies. Some authors have solved both undamped and damped torsional vibration problems by first converting the mechanical system into an equivalent electrical circuit. The equivalent circuit is then either built and tested or analyzed to determine its dynamic characteristics. The results, in terms of voltages and currents, are then converted back into their mechanical equivalents. McCann and Bennett [12] and Pollard [13] both illustrate the use of this method.

Uncommon electrical machines. The discussion will be limited to the motor and generator types most often found in turbomachinery. Specifically, DC and three phase AC machines will be the only types addressed. Additionally, all discussion of synchronous motors will refer to those having rotors with salient poles. The user who encounters a machine not mentioned herein is strongly advised to consult with the manufacturer for torsional vibration characteristics.

Measurement of torsional vibration. This paper is primarily concerned with the design and analysis process so testing procedures are not addressed. Additionally, like many of the other topics on this list, the subject of measuring devices and techniques is worthy of a paper of its own. Simmons and Smalley [14], Hershkowitz [15], and Wachel and Szenasi [16] all provide detailed descriptions in this area.

Electrical circuit damping. Only mechanical sources of damping are discussed herein. These include damping that occurs in electric motors and generators due to their torque *vs* speed characteristics. However, any damping that occurs due to electrical control circuits varying the excitations to electrical machines is well beyond the scope of this presentation. The interested reader should see Hammons [17].

Subsynchronous resonances in turbogenerators. There have been a slew of papers written on this relatively rare phenomenon, which is characterized by resonant interactions between the electrical network and the mechanical drive train. In order to evaluate this potentially destructive mechanism, a comprehensive model encompassing both the network and drive train must be utilized. A description of the steps required to prepare and run such a model would be worthy of a tutorial of its own. A substantial list of references on this complex subject is provided in a 1992 article [18].

Malsynchronization of synchronous motors and generators. If the electrical control circuits are not designed properly, malsynchronization can occur and generate pulsating torques that are many times the machine's rated torque. The consequences of this are often catastrophic. However, since this effort is written primarily for mechanical engineers, this subject is not covered. The user is advised, however, to maintain effective communication with the cognizant electrical engineers during the entire design process to avoid potential problems. Further elaboration on this topic is provided by Rana and Schulz [19], Joyce, et al. [20], and Undrill and Hannett [21].

UNDAMPED ANALYSIS

The first step in any torsional analysis procedure is determination of the system's natural frequencies and mode shapes. To accomplish this, a lumped parameter model, consisting of disk and shaft elements, is usually generated. The disks represent the system's significant inertial components while the shaft elements behave as torsional springs. All springs are assumed to behave in a linear fashion such that the torque they exert is directly proportional to their twist angle. A schematic representation of a three disk, two shaft model is presented in Figure 3.

Since real systems contain energy dissipation elements, known as dampers, along with inertia and stiffness elements, these technically also should be included in Figure 3. However, the addition of damping makes the determination of natural frequencies considerably more difficult. Additionally, the vast majority of the available literature concedes that the error introduced by ignoring damping in the calculation of natural frequencies is practically negligible. Thus, all natural frequencies and mode shapes discussed herein will be those associated with the undamped system.

The number of degrees of freedom possessed by the system is equal to the number of disks in the model. Any system, such as that of Figure 3, which does not have a shaft element connected to ground has a trivial natural frequency of zero, representing the case

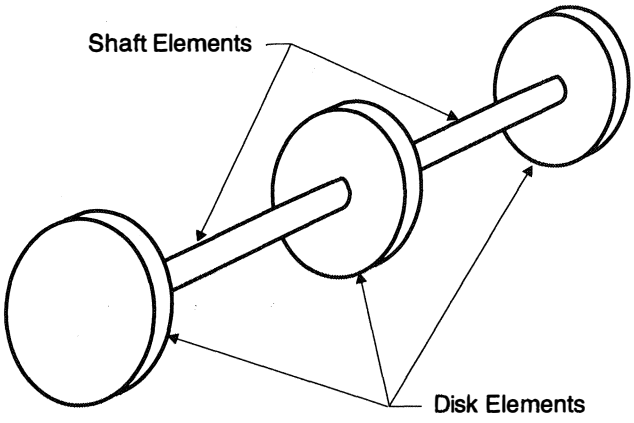

Figure 3. Three Disk Torsional System.

where all elements rotate together as a rigid body. The number of nontrivial natural frequencies that can be obtained for such a system is, thus, one less than the number of disks in the model.

Each natural frequency has an associated mode shape which describes the shape the shaft twists into during free vibration. A representative mode shape is shown in Figure 4. The abscissa values represent the axial positions of the disk elements while the ordinates correspond to the angles of twist occurring at each disk. As is the case with lateral vibrations, it is meaningless to refer to absolute displacements since they are theoretically infinite. The only information that can be obtained from a mode shape is the relationship between the displacements at the various disks. Accordingly, these curves are arbitrarily normalized such that the system's maximum displacement is equal to one radian. Mode shapes are often referred to as normal to reflect the fact that they are all orthogonal to each other.

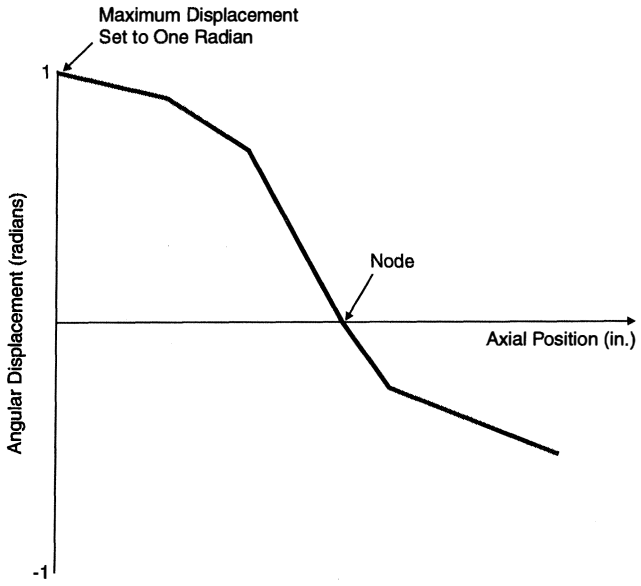

Figure 4. Representative Mode Shape.

The natural frequency associated with a particular mode shape can be easily identified by counting the number of nodes in the mode shape plot. Nodes are points that undergo zero deflection and are located at all points where the mode shape plot crosses the x-axis. The lowest natural frequency is known as the fundamental and has a mode shape with only one node, as is illustrated in Figure 4. Likewise, the second mode contains two nodes, the third has three, etc.

Prior to describing the analysis procedure, it should be noted that natural frequencies are properties of the entire system. If any component is changed, the torsional characteristics can be drastically altered. Thus, whenever a system is changed, a new torsional analysis should be performed. Additionally, since torsional response is a system property, nothing is gained by analyzing the individual components by themselves.

Modelling

The first task to be accomplished in the analysis procedure is generation of the lumped model. Firstly, all significant inertias in the system should be identified as disks. These include impellers, propellers, motor and generator rotors, gears, and coupling hubs.

The choice of the number of disks to include is usually a compromise. If every single inertia that exists in the assembly were represented, the modelling and solution time would likely be prohibitive. On the other hand, if complex turbomachinery trains were modelled as two disk systems, as was suggested in the INTRODUCTION section, the loss of accuracy would probably be unacceptable.

Another consideration is that the number of natural frequencies that can be calculated is limited by the number of disks in the model. The analyst must ensure that enough disks are included such that all natural frequencies that could reasonably be expected to be excited within the machine's operating speed range are determined.

All disk elements must be assigned a value for mass polar moment of inertia. The inertias for components bought from vendors such as electric machines and couplings can usually be obtained from the manufacturer. The remaining inertia values are generated either by test or calculation. The classic works by Ker Wilson [2] and Nestorides [8] present equations for the inertias for disks of almost every conceivable configuration. Continuously distributed inertias may require the use of numerical integration.

The most common inertia element, a hollow disk, has an inertia given by the following:

$$J = \rho \bullet \pi / 32 \bullet (D_o^4 - D_i^4) \bullet L \qquad (1)$$

where:
J = Mass polar moment of inertia (lbm−in^2)
ρ = Material density (lbm/in^3)
D_o = Outside diameter (in)
D_i = Inside diameter (in)
L = Length (in)

Once the inertias are determined, the torsional spring rates for the shaft sections which interconnect the disks must be found. The general equation for the torsional stiffness of a shaft is as follows:

$$k = G \bullet I_p / L \qquad (2)$$

where:
k = Torsional stiffness (in−lbf/rad)
G = Shaft material shear modulus (psi)
I_p = Area polar moment of inertia (in^4)
L = Length (in)

Once again, Ker Wilson [2] and Nestorides [8] provide equations for virtually every shaft configuration to be found in practice.

Since the model is the foundation upon which the entire analysis procedure is based, it is imperative that it represent the actual machine accurately. General guidelines for generating good models are as follows:

• Disk elements are usually axially located at the center of gravity of the impeller that they represent.

• If a disk element is extremely rigid, the portion of the shaft that lies within that element is assumed to have zero deflection. Shaft element lengths are, thus, calculated up to the face, not the centroid, of such an impeller.

• If a disk element is not extremely rigid, its stiffening effect on the shaft carrying it is modelled by assuming that the shaft ends at what Nestorides [8] calls a point of rigidity within the impeller. As is illustrated in Figure 5, the shaft is assumed to deflect in its normal fashion up to this point. Beyond this point, there is no deflection. Nestorides [8] provides equations for locating the point of rigidity for several common configurations.

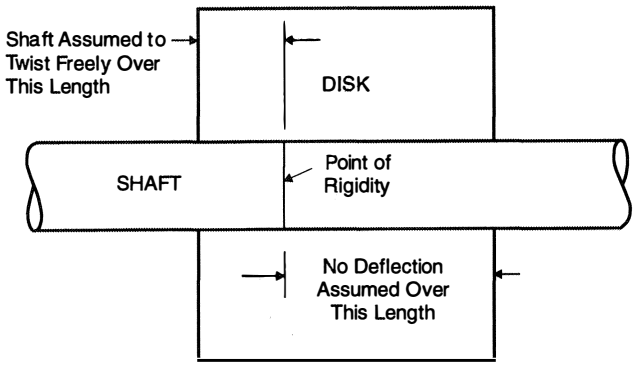

Figure 5. Point of Rigidity.

• When a shaft is joined to a nonrigid coupling or impeller by an interference fit, the shaft should be assumed to twist freely over a length equal to one-third of the overlap. The remainder of the overlap should be assumed rigid.

• When a shaft is joined to a nonrigid coupling or impeller by a keyed joint, the shaft should be assumed to twist freely over a length equal to two-thirds of the overlap. The remainder of the overlap should be assumed rigid.

• Utilization of some solution algorithms requires that shaft elements be assumed massless. If this is the case, it is usually sufficient to apply one-half of the actual shaft inertia to each of the disks on either end of the shaft element. However, if the inertia of a shaft element turns out to be of a comparable magnitude to those of the major disks in the system, a more accurate procedure is called for. In this case, it is best to divide the shaft element into a number of disk and shaft elements, with each disk representing a portion of the shaft's inertia.

• Couplings should be modelled as a shaft having the coupling's spring rate between two disks whose inertias are each equal to one-half of the coupling's total inertia.

• Flanges should be treated as shaft elements having diameters equal to their bolt-circle diameters.

• When a distributed inertia is divided up into shaft and disk elements, the accuracy of the model increases with the number of elements.

• Although gear teeth have inherent flexibility, for most practical cases, they can be considered to be torsionally rigid. In general, gear tooth flexibility is significant only in the calculation of very high natural frequencies or when a system contains multiple gear meshes. If it is desired to account for tooth flexibility, Nestorides [8] should be consulted for the appropriate equations.

• Disks that represent propellers operating in water should have their inertias increased to account for the mass of the entrained water. Ker Wilson [2] gives the following equation for the inertia of the fluid:

$$J_f = .25 \bullet J_p \bullet PR \tag{3}$$

where:
J_f = Inertia of entrained fluid
J_p = Dry inertia of propeller
PR = Propeller pitch/diameter ratio

Although the same correction should probably also be made for pump impellers, there are no reliable methods, other than the use of test data, that the authors are aware of. The authors have often merely used the dry inertias without encountering any problems.

Geared Systems

When creating models, systems containing gear meshes require special handling. Since all of the various shafts run at different speeds, to facilitate solution, it is customary to convert the elements' parameters to the equivalent values that they would have if they were all on the lowest speed shaft. The resulting equivalent single shaft model has exactly the same dynamic characteristics and natural frequencies as the actual system. The concept of equivalent values is analogous to the common practice of combining electrical resistors or mechanical springs in series or parallel to obtain an equivalent resistance or spring rate.

The use of an equivalent system assumes that the meshing gears rotate together without separation throughout the entire vibratory period. Assuming no separation means that each gear mesh contributes only one degree of freedom to the system, despite the fact that there are two disks in each mesh. For a given gear mesh, the parameter values for elements on the low speed shaft are unchanged. However, elements on the high speed shaft must be transformed via the following equations:

$$J_{eq} = J \bullet N^2 \tag{4}$$

$$k_{eq} = k \bullet N^2 \tag{5}$$

where:
J_{eq} = Equivalent inertia referenced to low speed shaft
J = Actual inertia
N = Gear ratio ($N > 1.0$)
k_{eq} = Equivalent stiffness referenced to low speed shaft
k = Actual stiffness

The above equations are utilized, one gear mesh at a time, to replace two shafts by an equivalent one. The parameters for the high speed shaft are all increased by the square of the gear ratio to reflect the larger energy levels they operate at. The equivalent elements are axially located on the equivalent shaft in the same positions they occupy in the actual arrangement. Equations (4) and (5) are used sequentially on each gear mesh in the assembly until all parameters have been referenced to the lowest speed shaft in the system. Once a single equivalent shaft has been obtained, any of the well known solution procedures, which will be discussed shortly, can be implemented.

Nonlinear Couplings

Many couplings that include rubber elements to provide damping have decidedly nonlinear stiffness characteristics similar to those shown in Figure 6. The effective spring rate, which is the slope of the curve, is, therefore, a function of the applied torque and angle of twist. This nonlinear feature makes the calculation of natural frequencies a somewhat more difficult task.

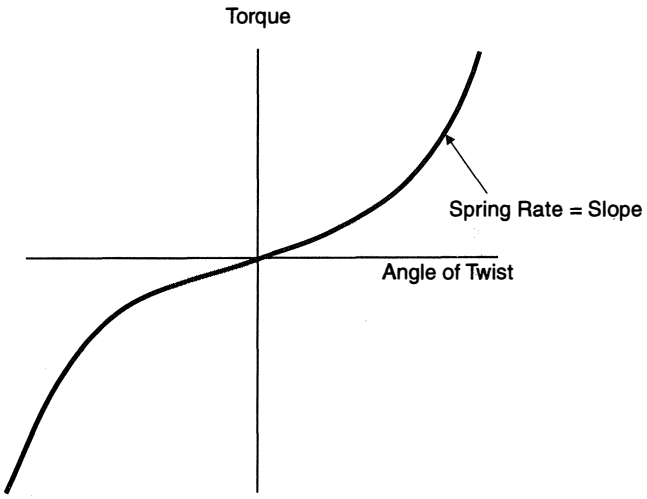

Figure 6. Nonlinear Coupling Behavior.

To overcome this difficulty, the authors recommend utilization of a technique provided by Andriola [22]. The method consists of converting the coupling's torque *vs* displacement curve into a curve of coupling spring rate *vs* shaft speed, as is illustrated in Figure 7. Since the spring rate is the instantaneous slope of the torque-displacement curve, its relationship to transmitted torque is known. A curve similar to Figure 7 can then be generated using the load's torque-speed characteristic.

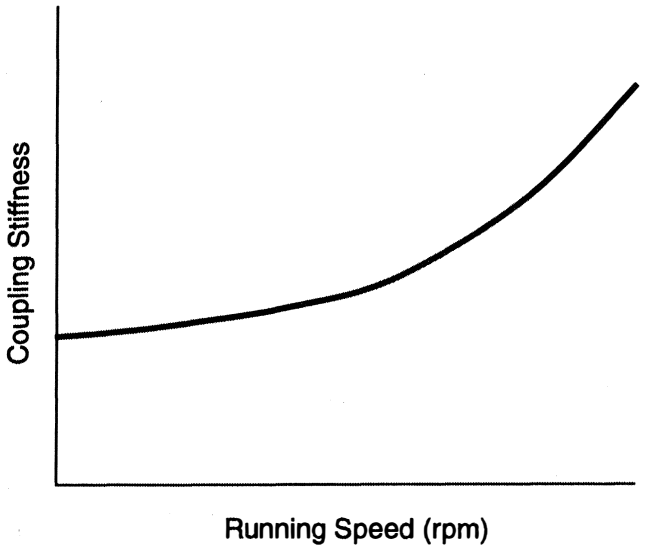

Figure 7. Nonlinear Coupling Stiffness Vs *Speed Relationship.*

Once the relationship between spring rate and running speed is determined, then an iterative procedure is implemented to find the natural frequencies. The steps to be taken are as follows:

- Guess a value for the natural frequency.
- Assuming a once per revolution excitation, calculate the running speed corresponding to that natural frequency.
- Using this speed and the curve of coupling spring rate *vs* running speed, determine the instantaneous coupling stiffness.
- Using this coupling stiffness, calculate the natural frequency.
- If the calculated natural frequency matches the guess value, a solution has been found. If not, go back to the beginning and try another guess value.

This procedure is repeated until all natural frequencies have been found. Obviously, the higher natural frequencies will not have a 1× running speed that lies within the operating range. These frequencies should have their corresponding running speed calculated using 2× excitations or the lowest order number excitation that is appropriate.

It is seen that the presence of the nonlinear coupling causes the system's natural frequencies to be dependent on speed, as is often the case in lateral systems. The above procedure assumes that the natural frequency is the value that occurs at the speed where resonance with the lowest order excitation possible occurs. These are the most important natural frequency values since low order excitations are the ones most likely to cause problems in the field.

Hydraulic Couplings

Another component that requires special attention when modelling is the hydraulic coupling. Hydraulic couplings consist of two radially vaned impellers that are mechanically independent of one another. Torque is transferred from the driving to the driven shaft via kinetic energy of the working fluid. Accordingly, these devices are also called hydrokinetic couplings.

For any operating condition, the torques carried by the two shafts are identical. Since the coupling cannot transmit power at 100 percent efficiency, a slight reduction in speed occurs across the coupling. This reduction is referred to as slip and typical values are from one to three percent of the driving shaft's speed. The slip percentage is generally independent of operating speed and varies inversely with the transmitted torque.

By virtue of the speed difference, the fluid in the driving impeller is subjected to a higher centrifugal force than that in the follower. A circulating flow pattern is, thereby, established in the coupling. Flow moves outwards in the radial passages of the driver and inwards in those of the follower. This circulating flow is the essential mechanism by which torque transmission transpires.

Hydraulic couplings are sometimes used as speed reducers. In general, they can be designed to yield virtually any speed ratio between the two shafts, with the restriction that the driving shaft's speed must be the higher of the two. As noted previously, unlike geared reducers, the two shafts experience equal torques. There is, thus, no need to reflect inertias and spring rates across the coupling by the square of the speed ratio.

With regards to modelling, a review of the literature uncovered a nearly unanimous opinion that hydraulic couplings should be treated as zero spring rate elements that effectively divide the assembly into two independent torsional systems. The lone dissenting voice, however, was that of Ker Wilson [2], hardly one to be treated lightly. He claims that the zero spring rate model is only an approximation since, in reality, restoring forces in the fluid yield a small but finite spring rate. These restoring forces are generated by centrifugal forces in the fluid and are, therefore, proportional to the square of running speed. He provides the following equation for effective stiffness:

$$k_h = D^5 \bullet RPM^2 / 585 \qquad (6)$$

where:
k_h = Hydraulic coupling spring rate (in−lbf/rad)
D = Outside diameter of coupling impellers (ft)
RPM = Speed of driving member (rpm)

Thus, when modelling assemblies containing hydraulic couplings, the user has two options. Firstly, the machine can be treated as a single entity and the above equation can be utilized to determine the coupling's effective stiffness. On the other hand, the coupling can be assumed to have zero stiffness and the two resultant systems can be modelled separately. Even Ker Wilson [2]

acknowledges that the latter treatment is usually satisfactory for practical systems.

Analysis Methods

In this section, methods for calculating a system's torsional natural frequencies are described. This section is intentionally made brief because, in the authors' experience, determination of the natural frequencies is usually not a problem for most turbomachinery users. It is in the later utilization of this information where most users encounter difficulties and the paper's main thrust is directed accordingly.

As stated previously, the natural frequencies of a system are the frequencies that it can vibrate at indefinitely, in the absence of damping, without any external forcing function applied. The essential method for obtaining natural frequencies is similar to those used for any generic spring-mass system. Equations of motion are written for every disk in the system, using Newton's laws. Only spring and inertial torques are involved since there are no external torques and damping is ignored. The motion of each disk is then assumed to be perfectly sinusoidal, as follows:

$$\theta = \theta_o \bullet \sin \omega t \tag{7}$$

where:
θ = Angular position of a given disk as a function of time
θ_o = Amplitude of angular vibration
ω = Angular frequency (rad/sec)
t = Time (sec)

This assumption implies that all disks vibrate in phase with each other which is known to be true for undamped free vibration. Equation (7) is then differentiated twice and the results are substituted into the original equations of motion. The values of ω that solve these equations are the natural frequencies.

Utilization of the above method is straightforward when dealing with very small numbers of disks. For example, the simplest system imaginable, consisting of a single disk attached to a grounded spring, can be shown to have the following natural frequency:

$$\omega_n = (k / J)^{.5} \tag{8}$$

where:
ω_n = Natural frequency (rad/sec)
k = Torsional spring rate (in−lbf/rad)
J = Mass polar moment of inertia (lbf−in−sec^2)

This is seen to be of identical form to the natural frequency equation for a simple linear mass-spring system. It is seen that inertia is analogous to mass and torsional stiffness is analogous to linear spring rate.

The next basic system contains two disks separated by a single shaft, as was shown in Figure 1. The natural frequency for this system is:

$$\omega_n = (k \bullet (J_1 + J_2) / (J_1 \bullet J_2))^{.5} \tag{9}$$

The above procedure has been used for other combinations of shafts and disks and the resulting equations can be found in many introductory vibration texts. However, once the number of degrees of freedom exceeds three, closed-form solutions, if available, become extremely unwieldy. For such systems, other methods should be utilized.

Holzer's Method

Probably the most well-known procedure for analyzing torsional systems is Holzer's method. The basis of this method is that free vibration can occur with no external torques acting on the system only if the vibration frequency is a natural frequency of the system. In this procedure, a guess value of frequency is selected and a Holzer table is generated. The table is started by assuming that the first disk in the system vibrates with the arbitrary amplitude of one radian. The torque required to generate this vibration is supplied by the adjacent shaft and is calculated and tabulated. Each disk is then sequentially looked at and the torque in the shaft behind it required to sustain vibration is calculated.

These calculations are continued until the last disk is reached. This disk, of course, has no shaft behind it. Thus, the torque required to keep this disk in motion reveals the system's mode of vibration. If this torque is positive or negative, it must be supplied by an external source and the system can only execute forced vibration at the guessed frequency. However, if this torque is zero, the system is in free vibration and the guessed value is a natural frequency.

The above procedure is repeated with various guess frequency values until the desired natural frequencies are found. Each guess value for the natural frequency requires its own Holzer table. The curve presented in Figure 8 is utilized to choose successive guess values and zero in on the natural frequency. This curve is a generic plot of the torque required to vibrate the system's last disk, known as the residual torque, *vs* the guessed value of natural frequency. All frequency values where the curve crosses the x-axis are natural frequencies. It is seen that odd natural frequencies are approached from positive residuals and even ones from negative residuals. The analyst, thus, knows in which direction to move the guess value based on the sign of the residual torque. For instance, if the second natural frequency is being sought and the residual torque resulting from the last guess is positive, the next guessed frequency should be made lower.

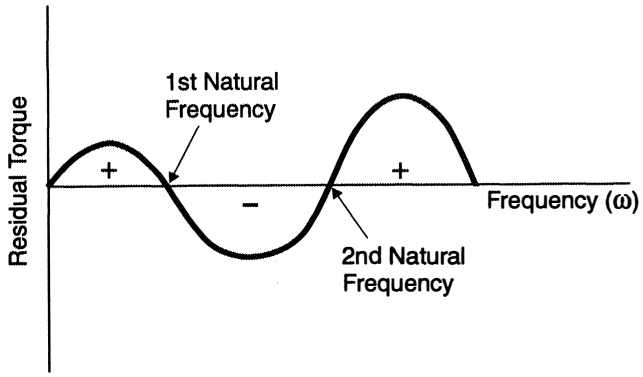

Figure 8. Residual Torque Behavior in Holzer's Method.

The mechanics for generating Holzer tables are explained in detail in Den Hartog's classic book [23] and many other vibration texts and are omitted here. However, it should be noted that once a natural frequency is found, the cognizant table contains other useful information including the mode shape, the inertial torque acting on each disk, and the angle of twist in each shaft.

Holzer's method lends itself very nicely to programming on a digital computer. Computers can proceed through the mechanics and perform the necessary iterations virtually instantaneously. There are many natural frequency programs in existence today that are based on Holzer's method or variations thereof.

There are other popular procedures in existence that bill themselves as transfer matrix methods. Each shaft and disk element in a system has an associated transfer matrix which describes the relationship between the torques and displacements on either side of the element. Transfer matrix elements, therefore, are functions of

inertia, stiffness, and frequency. In these procedures, all of the individual element transfer matrices are multiplied together to obtain expressions for the torque and displacement of the last disk in terms of those at the first. Since this is essentially what Holzer's method does, transfer matrix methods can be considered as variants of Holzer's method.

Matrix-Eigenvalue Methods

Most other procedures used for undamped analysis today fall under the heading of matrix-eigenvalue methods. These methods are essentially the same as the basic method described for simple systems earlier since they also involve solution of the differential equations of motion. The only major difference is that matrices are utilized to simplify the math.

Matrix methods are begun by writing the equations of motion in matrix form. The general undamped equation is:

$$[k] \bullet [\theta] + [J] \bullet [\alpha] = [0] \tag{10}$$

where:
$[k]$ = Stiffness matrix
$[J]$ = Inertia matrix
$[\theta]$ = Angular displacement vector
$[\alpha]$ = Angular acceleration vector

Both the stiffness and inertia matrices are square matrices having the same number of rows as there are disks in the system. Additionally, the inertia matrix is diagonal. The stiffness and inertia matrices are generated from the known disk inertias and shaft spring rates. The two vectors have the same number of rows as the matrices and represent the displacements and accelerations of the individual disks. These are the unknowns to be solved for.

Once Equation (10) is generated, the next step is to assume simple harmonic motion as follows:

$$[\theta] = [\theta_o] \bullet \sin \omega t \tag{11}$$

The above is the matrix equivalent of Equation (7). Substituting the above into Equation (10), the so-called eigenvalue equation is obtained:

$$\{[J]^{-1} \bullet [k] - [\omega^2]\} \bullet [\theta] = [0] \tag{12}$$

where:
$[\omega^2]$ = Diagonalized eigenvalue matrix

Matrix methods, which can be found in many mathematics texts, are then used to find the eigenvalues. These are the values of ω^2 which satisfy the above equation. The natural frequencies are then obtained by merely taking the square roots of the eigenvalues. Associated with each eigenvalue is an eigenvector, $[\theta]$. These vectors provide the mode shape corresponding to each natural frequency. It should be noted that the assumption of no damping in the system results in the eigenvalues being purely imaginary and the eigenvectors being real.

As is the case with Holzer's method, there are many computer programs available which perform the above calculations. Regardless of which method is used, several experts estimate that the resulting natural frequencies are accurate to within three to five percent. This naturally assumes utilization of a reasonable model.

Results Verification

After the natural frequencies and mode shapes are obtained from the computer, many would consider the undamped analysis to be complete. However, the authors recommend taking one more step because computer solutions and analysts have been known to occasionally generate errors. Thus, the authors advocate that an independent hand calculation of the fundamental natural frequency be made to serve as a check for the computer analysis.

There are several means by which this hand calculation can be performed. The simplest case occurs when one of the couplings has a spring rate that is an order of magnitude lower than that of any of the other shaft elements. In this situation, which is not at all uncommon in turbomachinery, virtually all of the deflection in the fundamental mode will be taken in the springy coupling. The machine can then be approximated as a two disk system by simply adding together all of the inertias on each side of the coupling. Equation (9) can then be used to obtain the natural frequency.

The same basic procedure should also be utilized for more general systems. The basic objective is to reduce a complex system to a reasonable approximation that has three or less degrees of freedom. If this is done, a closed form equation like Equation (9) can be straightforwardly implemented.

Two basic principles are utilized in the reduction of systems. The first is that relatively small inertias have very little effect on the fundamental frequency. These disks should, thus, be ignored and the shaft elements on either side of them can be combined as springs in series. The second principle is that shafts having relatively large spring rates behave as if they were rigid in the fundamental mode. Therefore, these elements should be discarded and the inertias on either side of them can be added together.

In addition to comparison of the two fundamental frequency values, several other items can be used to validate the analysis. In systems that have a single weak link coupling, there should be a considerable gap between the first and second natural frequencies. Additionally, as stated above, the fundamental mode shape should have the majority of its deflection in the springy coupling and the node should be located somewhere in this vicinity. Furthermore, the displacements in a two disk system obey the following equation:

$$J_1 \bullet \theta_1 = J_2 \bullet \theta_2 \tag{13}$$

Thus, whichever side of the machine is represented by the lower inertia disk should exhibit more displacement in the fundamental mode shape.

For more general systems, the mode shapes can be checked to see if they obey the following equation which represents conservation of angular momentum:

$$J_1 \bullet \theta_1 + J_2 \bullet \theta_2 + J_3 \bullet \theta_3 + \ldots = 0 \tag{14}$$

Thus, with signs accounted for, the sum of the products of the inertias and their displacements should equal zero. This rule can be used to check any mode shape either by hand calculation or by eyeball.

If the above checks are utilized to validate the analysis, the user can be reasonably confident that the results are accurate. The undamped analysis can then be considered complete and the next step, generation of the Campbell diagram, can be taken.

GENERATION OF CAMPBELL DIAGRAMS

As was stated previously, one of the primary objectives of torsional vibration analysis is the identification of all potential resonant points. Since most practical systems have numerous natural frequencies and multiple sources of excitation, this is, by no means, a trivial task. A device which greatly aids in the determination of these points is the Campbell diagram (aka interference diagram). In addition, Campbell diagrams provide an excellent overview of the system's torsional vibration situation, analogous to the function provided by critical speed maps in lateral systems.

A Campbell diagram should always be generated as soon as the undamped analysis is completed. A representative diagram for an

ungeared system is depicted in Figure 9. The natural frequencies are plotted as horizontal lines and the operating speed range is designated by vertical lines. When plotting the speed range, the upper limit should represent the point where the overspeed trip system kicks in rather than the highest desired running speed. The upward sloping lines are harmonics of speed that represent the system's potential excitations. Intersections between these lines and the natural frequency lines that occur within the operating speed range are referred to as interference points and are indicators of potential resonances. There are two of these points illustrated in Figure 9. The speeds corresponding to interference points are known as critical speeds.

Although determination of the horizontal and vertical lines is rather straightforward, generation of the excitation lines requires considerable insight. There are many potential excitation sources which occur in common turbomachinery drive trains. Essentially, any mechanism which is capable of generating a periodic fluctuation in the system's transmitted torque is a potential excitation source.

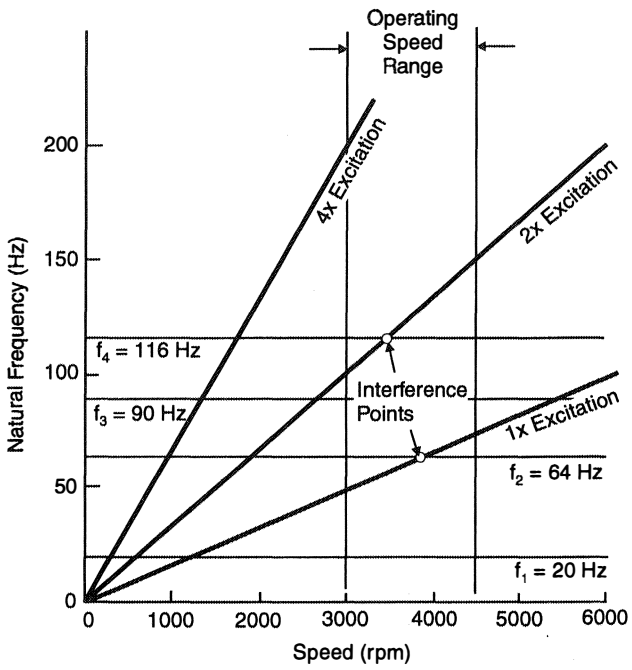

Figure 9. Representative Campbell Diagram.

In general, the excitations occur at integral multiples of the shaft speed. These multiples, which represent the number of vibrations which occur during each shaft revolution, are referred to as order numbers. For any given interference point, the order number is equal to the natural frequency divided by the critical speed, when each are expressed in the same units. Excitations having order numbers of one, two, and four are depicted in Figure 9.

Excitations

It is customary, as is shown in Figure 9, to use mismatched units in Campbell diagrams. The abscissas are usually expressed in rpm while the ordinates are in Hertz. Thus, generation of the excitation lines is not as straightforward as it would be if consistent units were utilized, since in that case the slope would be merely equal to the order number.

To generate an excitation line of a given order, a speed on the graph should be arbitrarily selected. The abscissa value for that speed should then be divided by 60 to convert the speed into Hertz. The ordinate is then obtained by multiplying the abscissa value in Hertz by the order number. Connection of this point with the origin by a straight line generates the desired excitation line.

The most common excitations are at once per revolution (1×) and twice per revolution (2×). These are generic sources that can arise via various mechanisms. 1× excitations can be generated by conditions such as rotating unbalance, eccentricity, and misalignment. Excitations of 2× are usually due to misalignment, ellipticity, or certain non-circular shaft cross-sections such as keyways. It is the standard practice of the authors to include both of these excitations in the analysis of all torsional systems.

In addition to these generic excitations, each system contains individual components that also generate excitations. In general, these sources include the system driver, such as a motor or turbine, and load, which is often an impeller. Additionally, all gear meshes are excitation sources. The various excitation sources will be specifically addressed in the text to follow.

Gear Excitations

Gears generate pulsations at several different frequencies. Errors in the generation of the gear teeth and in the mounting of the gear hub on the shaft can lead to unbalance, eccentricity, and/or misalignment. Such errors lead to fluctuations at a frequency of once per revolution of the cognizant shaft. Additionally, any errors that result in gear ellipticity generate torque variations at twice shaft speed. Thus, the generic 1× and 2× excitations previously alluded to must always be considered in gear meshes.

Furthermore, gears can produce disturbances at their meshing frequency and higher harmonics of it. For each shaft, meshing frequency is equal to the number of teeth on that shaft's gear multiplied by shaft rpm. These disturbances can be attributed to a phenomenon which Schlegel, et al. [24], refer to as engagement impulse.

Whenever a given tooth meshes, it inherits a portion of the load that had been carried by the previously engaged teeth. The removal of load from these teeth, which had been deflected by the loading, allows them to relax and spring back to their free position. This relaxation generates a tangential acceleration in the gear bodies which prevents the newly engaged teeth from meshing smoothly. The meshing is, therefore, impactive. As a result, an impulsive force is generated in each gear along their common line of action, causing the mesh's transmitted torque to pulsate each time a new tooth comes into mesh.

Whenever gears are present in a system, therefore, the interference diagram for each shaft should include three excitation lines. Their corresponding order numbers should be equal to one, two, and the number of teeth on that shaft's gear. Technically, excitations corresponding to higher harmonics of gear mesh frequency should also be included. However, all sources consulted dismiss these harmonics because of their negligible magnitudes.

Impeller Excitations

Another common excitation source is the vaned impeller which may act as either the load or the driver of the system. This category encompasses a wide variety of dynamic energy transfer devices including pump impellers, compressor and turbine rotors, and fans. In all of these devices, torque variations occur at blade-pass frequency due to pressure disturbances resulting from vanes passing a stationary object such as a volute or diffuser entrance. The order number for an impeller is, thus, equal to its number of vanes.

Additionally, impellers occasionally operate within casings that contain several equally spaced obstacles that can generate pressure fluctuations when passed by an impeller blade. Such a situation occurs in configurations employing vaned diffusers or volutes with multiple cutwaters. These casings can generate excitations having an order number equal to the number of stationary vanes or cutwaters.

Furthermore, it can be easily seen that disturbances can also be generated each time a rotor blade passes by a stationary vane or cutwater. The order number generated by this phenomenon is given by the following equation from Ker Wilson [2]:

$$n = N_r \bullet N_s / C_h \tag{15}$$

where:
n = Excitation order number
N_r = Number of blades on rotor
N_s = Number of stationary vanes or cutwaters
C_h = Highest common factor of N_r and N_s

Thus, a vaned impeller operating within a vaned diffuser can generate three separate excitations.

Propeller Excitations

Propellers behave in much the same fashion as bladed impellers. In marine applications, the reaction torque from the water varies each time a blade passes the ship's rudder. Thus, propellers also generate torque fluctuations at blade-pass frequency, although the fluctuations are usually much larger than in impellers. Propellers also create torque variations at integral multiples of blade-pass frequency but, by all accounts, they are usually negligible.

Electrical Machine Excitations

The pulsating torques that arise in electric motors and generators can be separated into two categories; those that occur when the machine is running at constant speed and those that transpire when the machine is accelerating or exposed to an electrical fault. Although both categories must be investigated during the analysis phase, the latter is the more likely to cause serious problems. Therefore, in contrast to all of the excitations addressed heretofore, electrical machine excitations are often of a transient nature.

In general, the best source of information regarding excitations produced by electric machines is the manufacturer. There are virtually an infinite number of designs for motors and generators and each one has its own unique excitation mechanisms. However, to familiarize the user with the more common excitation sources, some basic guidelines will be provided.

When running at steady speed, motors and generators can produce torque fluctuations via various mechanisms. Most AC motors and generators produce fluctuations at line frequency (60 Hz in the United States) and twice line frequency by a number of different phenomena. Thus, systems containing AC machines have horizontal excitation lines at line and twice line frequency. Additionally, many machines create oscillations having an order number equal to the number of magnetic poles in the machine.

In addition to the oscillations produced during steady running, AC machines generate torque fluctuations when subjected to short circuits across their terminals. These fluctuations also occur at line and twice line frequency. Although these excitations are of a transient nature, the magnitudes of the peak torques are usually many times the motor's rated torque. Because of this, most authors strongly advise avoiding natural frequencies near 60 and 120 Hz in assemblies containing AC motors or generators, if at all possible.

Another situation in which AC motors generate fluctuating torques is in the first instants after power is initially applied to them. Both induction and synchronous motors generate large transient torques at line frequency that die out rapidly. However, since the transients take much longer to decay in induction motors, they are far more likely to generate problems via this mechanism.

Thus, although the analysis of systems utilizing AC machines is anything but simple, the generation of the excitation lines on the Campbell diagram is relatively straightforward. In general, the excitations are at 60 Hz, 120 Hz, and sometimes at pole-passing frequency.

In addition to the above, AC synchronous motors also generate large pulsating torques at twice slip frequency during starting. The discussion of this unique phenomenon will be held off to a later section.

In general, DC machines generate excitations that are relatively small during steady operation. Additionally, when exposed to a short, DC machines merely experience an abrupt change in torque level. Unlike AC machines, there are no torque pulsations. There are many applications, therefore, where DC motors and generators are non-factors with respect to torsional vibration.

Variable Frequency Drive Excitations

All of the AC machines discussed so far have been assumed to operate at constant speed. These machines are supplied with a constant electrical frequency equal to line frequency. In contrast to these, many turbomachinery users are opting for the flexibility provided by variable speed motors. Such motors are controlled by variable frequency drives (VFD) which alter motor speed by varying the electrical frequency supplied to the motor's terminals. These drives represent an additional source of torsional excitation to be considered during the analysis phase.

Variable frequency drives contain a static frequency converter which electronically transforms the constant line frequency (60 Hz in the United States) to the desired electrical frequency for driving the motor. Since the speeds of synchronous and induction motors are essentially proportional to electrical frequency, any desired speed may be obtained by merely selecting the appropriate driving frequency. Most static converters are capable of producing electrical frequencies that are both above and below the supply frequency.

Most static converters consist of a rectifier in series with an inverter. The rectifier converts the AC signal at line frequency into a DC signal. The DC signal is then subsequently converted back into an AC signal at the desired frequency by the inverter. The outputs of the inverter are voltage and current waves that are very nearly sinusoidal. However, since they are not perfect sinusoids, periodic variations in the driven motor's output torque are created.

There are several different types of variable frequency drive in common usage today. The speed of induction motors is usually varied via control of the stator frequency. Pulse width modulators (PWM), voltage source inverters (VSI), and current source inverters (CSI) are popular devices that accomplish this. Synchronous motors are usually driven by load commutated inverters (LCI) which are similar to CSIs.

The excitation characteristics of the various devices that control stator frequency (PWMs, VSIs, CSIs, and LCIs) are practically identical. In these drives, the excitation frequencies are given by the following equation:

$$f_{ex} = n \bullet k \bullet f_e \tag{16}$$

where:
f_{ex} = Excitation frequency
f_e = Electrical frequency output by inverter
n = Number of pulses in converter
k = 1, 2, 3 ...

In both synchronous and induction motors, the motor speed is approximately related to the supplied electrical frequency by the following:

$$RPM = 120 \bullet f_e / N_p \tag{17}$$

where:
RPM = Motor speed (rpm)
f_e = Electrical frequency (Hz)
N_p = Number of poles in motor

The excitations are, therefore, upward-sloping lines whose order number is obtained by combination of Equations (16) and (17), as follows:

$$n_{ord} = n \bullet k \bullet N_p / 2 \quad (18)$$

The value of n is either six or 12 since all practical converters utilize six or 12 pulses. Since the number of poles must be an even number, the order numbers obtained from Equation (18) are always integers.

In contrast to the preceding devices, wound rotor induction motors are sometimes controlled by drives that Mayer [25] refers to as static Kramer drives. These drives are very different from those previously discussed since they do not alter the electrical frequency supplied to the motor's terminals. Instead, they control motor speed by varying the motor's slip. Unlike the other VFDs, whose excitation frequencies increase with motor speed, static Kramer drives act in the opposite direction. These drives produce pulsations at harmonics of the slip frequency, which is defined as follows:

$$f_s = f_l - f_e \quad (19)$$

where:

f_s = Slip frequency
f_l = Line frequency
f_e = Electrical frequency corresponding to motor speed

The generated harmonics are either multiples of six or 12, dependent on the number of pulses in the drive. The relationship between electrical frequency and motor speed is given by Equation (17).

In the speed range between zero and 10 percent of maximum speed, most variable frequency drives produce fluctuating torques that are several times larger than those generated over the remainder of the speed range. Because of this, most users choose to begin the active operating range at a speed above 10 percent. Thus, when induction motors are started, they behave in the same manner as in a fixed speed system since the variable frequency drive is kept out of the loop during starting. Once the speed reaches the operating region, the drive is activated and its torque pulsations are introduced to the system. Thus, in the interference diagram for such systems, the drive's excitations are shown only within the operating speed range, as is shown in Figure 10.

The above discussion generally applies only to induction motors. When synchronous motors are controlled via LCIs, the LCI is usually active throughout the entire starting process. The assembly must, therefore, endure the higher pulsating torques produced by the LCI in the low speed range. This is usually a transient condition, however, since the operating range is normally set above 10 percent speed.

In addition to the pulsations generated by the variable frequency drive, the normal fluctuations produced by AC machines are also present. When VSI class drives are employed, these pulsations occur at one and two times the electrical frequency across the motor's terminals. The order numbers for these pulsations can be obtained from Equation (18) using values of one and two for n and one for k. These excitation lines, thus, have shallower slopes than those produced by the VFDs. In systems using static Kramer drives, the pulsations merely occur at line and twice line frequency since the electrical supply frequency is not variable.

Synchronous Motor Startup Excitations

The majority of the preceding excitations transpire when the machine is running at constant speed. Any potential damaging interferences generated by them could be evaluated by a steady state forced vibration analysis. In stark contrast to these are the torque pulsations that are created by AC synchronous motors during the starting process. Interferences resulting from this phenomenon can usually only be evaluated via a transient forced vibration analysis.

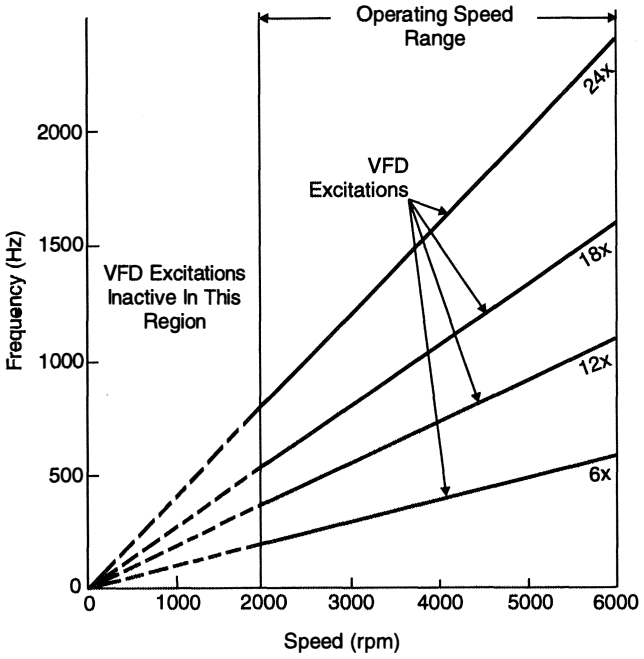

Figure 10. Variable Frequency Drive Excitations.

Unlike induction motors, synchronous motors are not self-starting. This is due to the fact that the stator's magnetic field begins rotating at synchronous speed virtually instantaneously after power is applied. With the stator field rotating and the motor at rest, alternating forward and reverse torques are applied to the rotor. This causes the rotor to swing back and forth by minuscule amounts and effectively prevents the buildup of any significant accelerations in either direction.

Since synchronous motors are not self-starting, they are normally equipped with squirrel-cage windings (aka amortisseur windings) which provide starting torque and also provide damping during steady state running. These windings are utilized to accelerate the motor as an induction motor from zero speed to a speed slightly less than synchronous speed. Starting is usually performed with no voltage applied to the rotor's field winding. When synchronous speed is approached, DC field voltage is applied and the rotor is pulled into synchronism.

Pulsating torques are created during this procedure due to the fact that synchronous motor rotors contain salient poles that are magnetic protrusions enclosed by field coils. The resulting asymmetry causes the motor's output torque to vary as a function of rotor position. This effect is in direct contrast to pure induction motors which have symmetric rotors and a generated torque that is independent of rotor location.

Synchronous motors are often modelled as having two axes of symmetry, the direct axis and the quadrature axis. The direct axis refers to a centerline that passes directly through one of the rotor's salient poles. When the direct axis is in perfect alignment with the magnetic field set up by the stator, the magnetic reluctance between rotor and stator reaches a minimum value. Accordingly, the torque generated in this position, known as the direct axis torque, represents an extreme (maximum or minimum) value produced during a revolution of the rotor.

On the other hand, the quadrature axis is a centerline which is perpendicular to the direct axis. The condition where this axis is

aligned with the stator's magnetic field represents the point of maximum magnetic reluctance. The resulting torque, which is referred to as the quadrature axis torque, represents the opposite extreme from the direct axis torque.

Accordingly, as the rotor rotates, the torque varies in a roughly sinusoidal fashion between the limits imposed by the direct axis torque and the quadrature axis torque. The mean value of these two torques is known as the average torque and represents the torque available to provide acceleration to the system. Superimposed on top of this torque is a pulsating torque whose magnitude is one-half the difference between the direct and quadrature axis torques. The various torque components are illustrated in Figure 11 as functions of speed for a hypothetical synchronous motor.

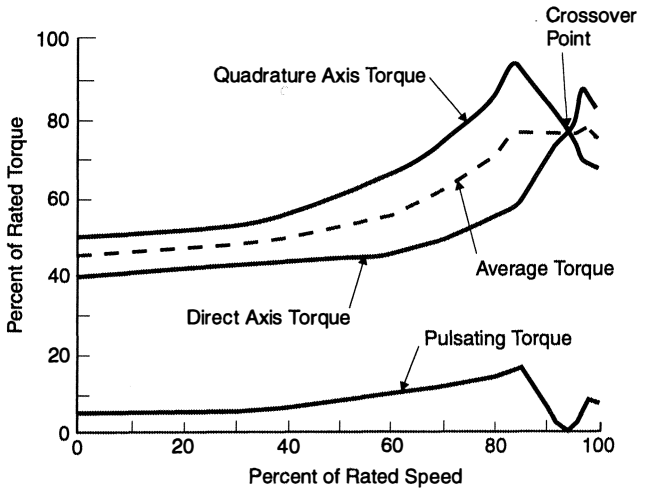

Figure 11. Synchronous Motor Torque-Speed Characteristics.

The frequency of the torque pulsations is the frequency at which the stator's rotating magnetic field passes a rotor pole. Since the stator's magnetic field rotates at synchronous speed, the excitation frequency is a function of the difference between synchronous speed and rotor speed, which is known as slip speed. Specifically, excitations occur at twice slip frequency where slip frequency is defined by the following equation:

$$f_{slip} = f_l \bullet (N_s - N) / N_s \qquad (20)$$

where:
f_{slip} = Slip frequency (Hz)
f_l = Line frequency (Hz)
N_s = Synchronous speed (rpm)
N = Rotor speed (rpm)

The motor's synchronous speed is given by the following equation:

$$N_s = 120 \bullet f_l / N_p \qquad (21)$$

where:
N_s = Synchronous speed (rpm)
f_l = Line frequency (Hz)
N_p = Number of poles

The ramifications of Equation (20) are extremely important. It is seen that the frequency of torque pulsations, twice slip frequency, decreases as rotor speed increases. Thus, at zero speed, the excitation frequency is equal to two times line frequency or 120 Hz in the United States. As the motor is accelerated, the excitation frequency decreases linearly until it reaches zero when the rotor achieves synchronous speed.

A Campbell diagram is presented in Figure 12 for a hypothetical system being driven by a synchronous motor. Synchronous speed is assumed to be 1800 rpm and all other excitations are omitted from this figure for clarity. It is easily seen that the motor generates interferences with all natural frequencies that are below twice line frequency, assumed to be 120 Hz.

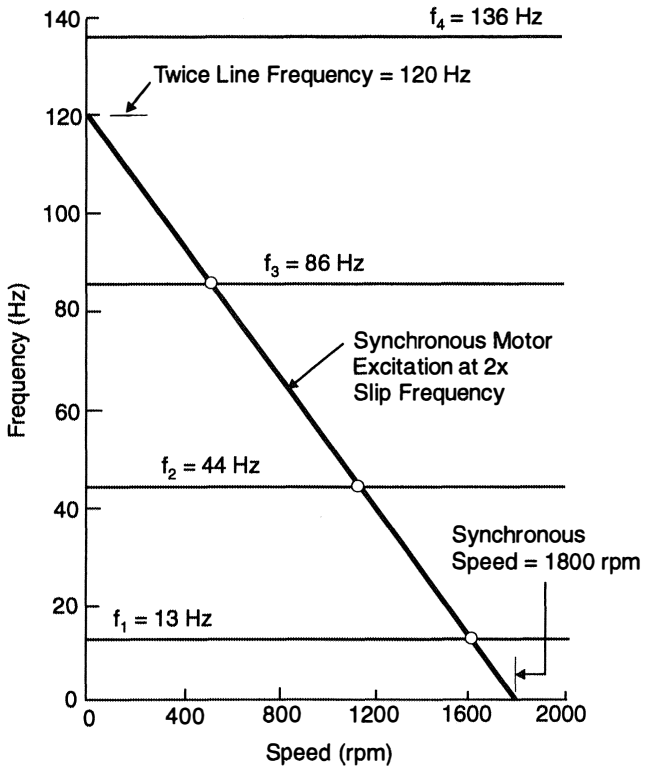

Figure 12. Synchronous Motor Campbell Diagram.

The results of Figure 12 are, by no means, unique to the example selected. In fact, most systems driven by synchronous motors will experience resonances with all natural frequencies below 120 Hz during starting. This is a significant source of potential problems since most practical turbomachinery drive trains have several natural frequencies within this range.

The discussion has so far been based on the assumption that the motor is started with no field excitation. If the user chooses to apply field excitation during starting, the pulsating torques at twice slip frequency are unchanged. However, an additional pulsation at slip frequency is introduced and the motor's average torque is reduced. Since both of these consequences are detrimental, almost all synchronous motors are started without field excitation and that shall be assumed henceforth.

Since the resonances occur only during starting, they are of a transient nature and, thus, may not be as troublesome as resonances occurring within the steady operating speed range. However, all interference points generated by synchronous motors must be investigated further using techniques to be discussed herein. The unique problems associated with analysis of synchronous motor-driven systems will be discussed in a later section.

It should be noted that the above discussion applies only to motors driven at line frequency. If a variable frequency drive is utilized in the system, the motor is in synchronism at all speeds. The twice slip frequency pulsations are, thus, absent. However, the pulsations produced by the drive must then be dealt with.

Geared System Example

The excitation frequencies generated by each of the discussed sources are summarized in Table 1. It should be noted that when an AC motor is driven by a VFD, the excitations generated by both the motor and the drive need to be accounted for. Once the relevant excitations are determined for a system, they should be plotted on a Campbell diagram to determine interference points. A hypothetical example will now be provided to illustrate the general procedure.

Table 1. Summary of Excitation Sources and Frequencies.

Excitation Source	Excitation Frequencies
Generic 1X (unbalance, eccentricity, misalignment, etc.)	One x Speed
Generic 2X (misalignment, ellipticity, etc.)	Two x Speed
Gear Mesh Consisting of Pinion with N_p Teeth Mating with Gear Having N_G Teeth	Pinion Shaft: • One x Pinion Speed • Two x Pinion Speed • N_p x Pinion Speed Gear Shaft: • One x Gear Speed • Two x Gear Speed • N_G x Gear Speed
Impeller with N_R Blades Rotating Inside Casing with N_S Cutwaters	• N_R x Speed • N_S x Speed • n x Speed (n is given by Equation (15)
AC Motor or Generator with N_p Poles (Fixed Frequency or Static Kramer Drive)	• Line Frequency (60 Hz) • Twice Line Frequency (120 Hz) • N_p x Speed
AC Motor with N_p Poles (Variable Frequency Drive Controlling Stator)	• $^1/_2$ x N_p x Speed • N_p x Speed
Variable Frequency Drive (Stator Frequency Control) with N Pulses Driving AC Motor with N_p Poles	• $^1/_2$ x N x N_p x Speed • N x N_p x Speed • 1.5 x N x N_p x Speed • 2 x N x N_p x Speed
Static Kramer Drive with N Pulses	• N x Slip Frequency • 2 x N x Slip Frequency
Synchronous Motor (Fixed Frequency Drive)	Two x Slip Frequency

It has been the authors' experience that the generation of Campbell diagrams for geared systems is a source of confusion for many users. To help to alleviate this, the example system consists of a motor and pump operating on two different shafts, as is shown in Figure 13. The motor is assumed to be a two-pole induction motor driven by a variable frequency six pulse VSI drive. The motor speed is assumed to vary between 1000 and 1800 rpm. The gear mesh provides a 2.5 to 1 ratio, resulting in a pump speed range of 2500 to 4500 rpm. The pump impeller is assumed to have eight blades while the pinion and gear tooth numbers are 10 and 25 respectively. The variable frequency drive is inactive at all speeds below the operating range.

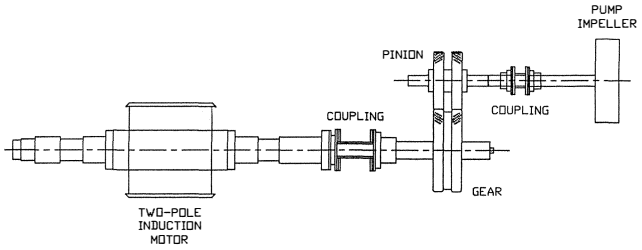

Figure 13. Example Motor-Driven Pump.

The undamped analysis is assumed to be complete and there are four natural frequencies within the range of interest. These occur at 50, 220, 340, and 500 Hz.

The first item to address in generation of the Campbell diagram is calculation of the order numbers for the motor and variable frequency drive. Since there are two poles in the motor, use of Equation (17) reveals that the speed in rpm is equal to 60 times the electrical frequency in Hz. Thus, the speed and electrical frequency are equal when expressed in consistent units. The induction motor pulsations, which occur at one and two times the electrical frequency, therefore, are represented as 1× and 2× excitations on the Campbell diagram.

The order numbers for the VFD are obtained by inputting six for n and two for N_p in Equation (18). The resulting excitations are, thereby, at 6×, 12×, 18×, 24×, etc. For the sake of clarity only the first three excitations will be utilized in the example Campbell diagrams.

The order numbers for the motor shaft are as follows:
Generic 1× excitation: 1
Generic 2× excitation: 2
Induction Motor excitation: 1, 2 (duplicates of the above)
Variable Frequency Drive excitation: 6, 12, 18
Gear mesh excitation: 25

The corresponding order numbers for the pump shaft are:
Generic 1× excitation: 1
Generic 2× excitation: 2
Impeller blade excitation: 8
Pinion mesh excitation: 10

There are several options for displaying the above on Campbell diagrams. Perhaps the simplest method is to prepare separate diagrams for each shaft, as is illustrated in Figures 14 and 15. The natural frequencies are the same on both diagrams since the gear ratio has no impact on them. The excitation lines are simply drawn at the slopes indicated by the above order numbers, which are all integers. Both diagrams are then checked for interferences.

It is seen from Figure 14 that there are six interferences, all designated by circles, occurring in the motor shaft. Likewise, the pump shaft generates four interference points. It must be remembered that any interference found on one shaft's diagram can cause vibration problems in the other shaft since the two shafts are assumed rigidly connected at the gear mesh.

Another method of handling the example system is to plot all information on a single interference diagram, as is shown in Figure 16. In this case, both motor and pump speed ranges are indicated on the diagram. All excitations are plotted on the figure at their actual slopes. A problem that arises from this method is the apparent indication of false interference points. An example of this is intersection point B, between the second natural frequency and the 8× line representing impeller blade excitation. Since this point is located within the motor speed range, it appears to be a bona fide interference point. However, when it is remembered that the 8× excitation is only related to pump speed, it is seen that this point is meaningless. Likewise, points C, D, and E are also invalid. Because of the large potential for this type of confusion, the authors do not recommend the use of this method.

A much better method of plotting all of the relevant information on one diagram is illustrated in Figure 17. In this diagram, everything has been referenced to motor speed. The motor excitations are drawn in the same manner as in the previous plots. However, all excitations acting on the pump shaft must have their order numbers multiplied by the gear ratio in order to be referenced to motor speed. For instance, the generic 1× excitation on the pump shaft is drawn with an order number of 2.5. The other pump shaft excitations are represented as 5×, 20×, and 25× lines.

Comparison of Figure 17 with Figures 14 and 15 reveals that the two methods yield the same interference points. For instance, point A in Figure 15 is an interference with the fundamental mode at a pump shaft speed of 3000 rpm. Point F of Figure 17 occurs at a

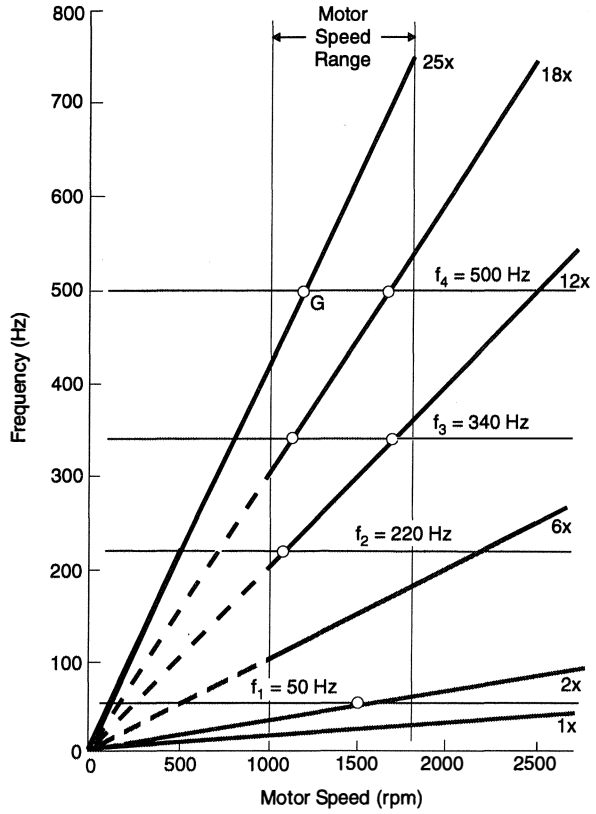

Figure 14. Motor Campbell Diagram.

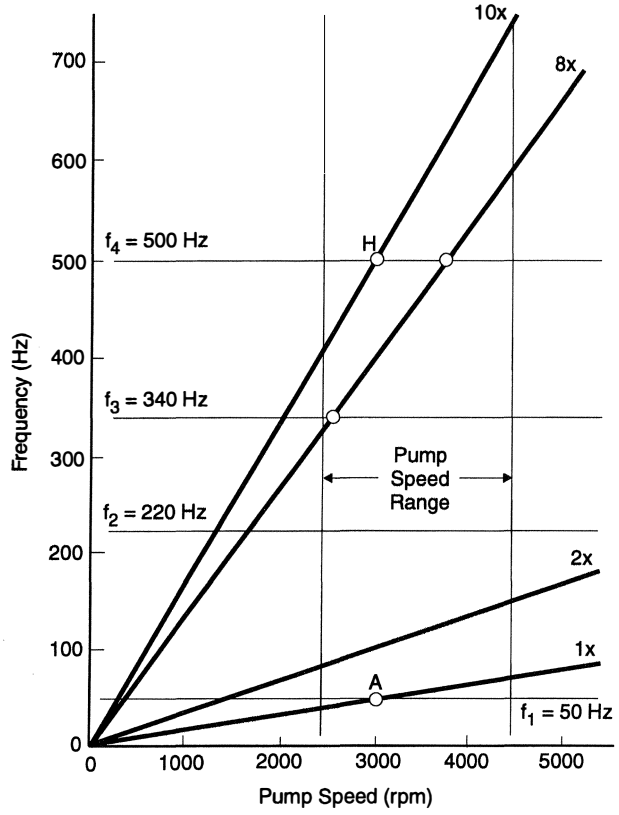

Figure 15. Pump Campbell Diagram.

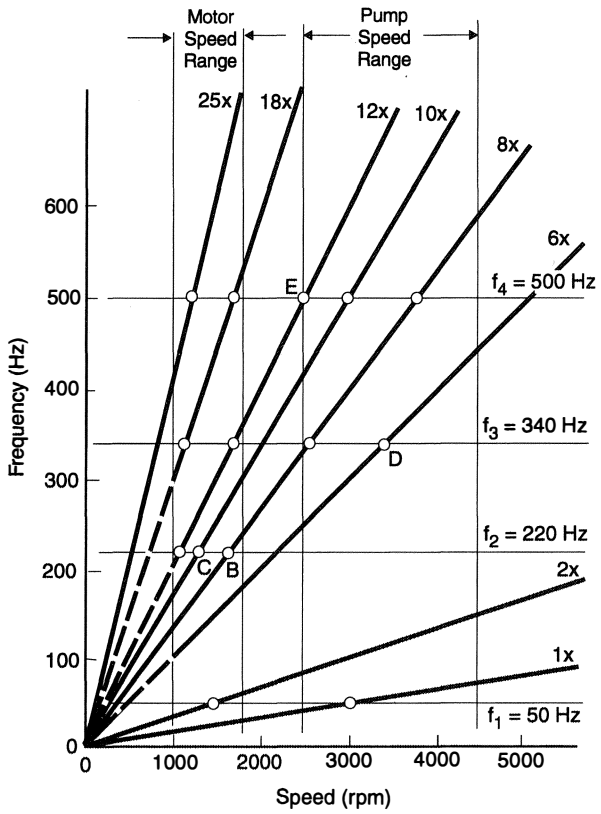

Figure 16. Combined Motor/Pump Campbell Diagram.

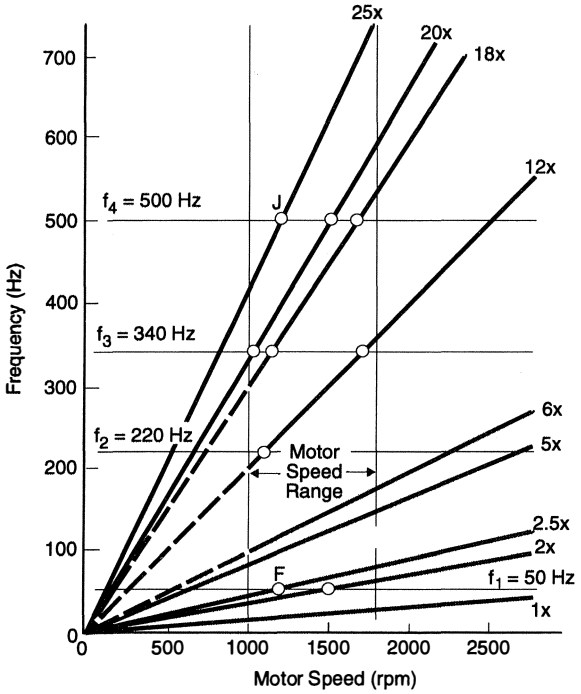

Figure 17. Combined Motor/Pump Campbell Diagram.

motor speed of 1200 rpm which is equivalent to a pump speed of 3000 rpm. The two points are, thus, identical.

The reader might notice that there are a total of 10 interference points in Figures 14 and 15 while Figure 17 contains only nine. The explanation for this is that point G from Figure 14 and point H

in Figure 15 both represent interferences where the fourth natural frequency is excited by the gear meshing frequency. These points are, thus, redundant and are represented by a single point, point J, in the combined diagram. Thus, the procedure of Figure 17 is perfectly acceptable as long as the introduction of non-integral order numbers doesn't bother the user from an aesthetics standpoint.

INSPECTION OF INTERFERENCE POINTS

After the Campbell diagrams are completed, the next step in the analysis procedure is the identification of intersections between natural frequency and excitation lines that represent true interferences. The statement made previously that intersection points that occur within the operating speed range are the only ones considered to be interferences is not entirely true. After all, an intersection point shown by analysis to lie just outside of the speed range could, in actuality, be within the range if the analysis contained inaccuracies.

In order to prevent the erroneous elimination of intersection points, the margin between the intersection point and the top or bottom limit of the speed range should be calculated using the following equation:

$$MAR = \delta N / N_1 \bullet 100 \qquad (22)$$

where:

MAR = Margin (percent)
N_1 = Top or bottom limit of speed range (rpm)
δN = Difference between speed at intersection point and N_1 (rpm)

Once the margin is determined, the question arises as to how much margin is required to eliminate a potential interference point. To a certain extent, this is a matter of judgment. Obviously, one percent is insufficient since the accuracy of the natural frequency calculation is no better than three to five percent. On the other hand, few analysts would be concerned if a 50 percent margin were demonstrated.

The API codes for pumps, compressors, and turbines specify a minimum margin of 10 percent between operating speed and intersection point speed. A survey of the available literature reveals a general consensus that the allowable margin should be somewhere between 10 and 20 percent which is consistent with the authors' experience. In general, the authors require a minimum margin of 15 percent. Under special circumstances, the authors have permitted mild deviations to this rule but under no circumstances would they condone a margin of less than 10 percent.

Once the required margin has been decided upon, all intersection points unable to meet the requirement should be identified as interference points. To these points should be added all transient intersection points generated by synchronous motor and variable frequency drive excitations.

Once the true interference points have been determined, the user generally has two choices for dealing with them. Either design changes, such as alteration of couplings, are implemented to eliminate the interferences or the interference points are subjected to further analysis. Since the first alternative is often costly and/or impractical, the authors recommend that the second course be followed.

The further analysis route can sound daunting to the uninitiated user since forced, damped analyses are often relatively time-consuming. If the fact that systems often contain many interference points, as is the case in Figure 17, is also considered, the analysis alternative may appear to be totally impractical. Fortunately, many interference points can be dismissed from consideration by mere inspection. In the procedure advocated herein, all interference points are subjected to inspection and only those that are not eliminated in this step undergo further analysis.

The first step of the inspection procedure is the tabulation of all interference points. For all points, the following three items should be noted:

- Excitation source
- Running speed
- Normal mode which undergoes excitation

The basis of the inspection method is that the only undesirable effects of torsional resonance are large cyclic torques and stresses. Unlike lateral vibration, the vibration amplitudes are normally not a concern. Thus, the major concerns are of a structural nature. If the induced cyclic torques are large enough to cause a gear mesh or coupling to be overloaded, the situation is unacceptable. Additionally, if the cyclic stresses are large enough to cause fatigue failure of a shaft, then there is a problem. Furthermore, if torque reversals occur at gear or spline interfaces, there could be a problem. However, any resonant point that does not lead to one of those three situations can generally be dismissed from consideration.

With the above criteria in mind, the first thing the analyst should do is look at the amplitude of free vibration, as revealed by the mode shape, at the location of the excitation torque. Since there are usually multiple locations where the generic 1× and 2× excitations can occur, this process applies primarily to fluctuations arising from a specific source such as a motor, gear mesh, or impeller. If the mode shape reveals that the excitation source is located near a node, the excitation will have virtually no effect on the system. Any interference point having this characteristic can be immediately dismissed.

The above rule applies when the excitation is in the form of a pulsating torque, which is the type of excitation generated by all components discussed herein except for gears. As will be described later, gears can generate two very different types of excitations, torques and displacements. Gear torque excitations behave in exactly the same manner as all other torque excitations and are, thus, subject to the above rule. However, displacement excitations are radically different in that they are most effective when located at nodes. Therefore, they cannot be eliminated on the basis of the above argument.

The mode shape can also be used to select only one point to be analyzed for the case where a specific mode is excited by more than one source. In general, the effectiveness of a given excitation is a strong function of its amplitude in the mode shape. Thus, if one point has an excitation located at a point of much higher amplitude than the other points, that point will result in the worst case cyclic torques and stresses, as long as the excitation torque magnitudes are about equal. The worst case interference point would then be submitted to a forced vibration analysis but the remaining points could be ignored. Once again, this rule applies only to torque excitations.

A third way in which the mode shapes can be of assistance is by their indication of the relative magnitudes of induced torques at various locations. In general, the largest cyclic torques will occur in shaft regions exhibiting the most twist, or highest slopes, in the mode shape. These regions are usually at or near nodes. Therefore, if a system had a region which was an unquestionable weak link, such as a quill shaft, interference points having a shallow slope in this region could probably be safely eliminated.

Another element that should be accounted for is the torque *vs* speed characteristic of the driven load. In many turbomachines, such as centrifugal pumps, the transmitted torque is proportional to the square of the operating speed. Therefore, if a given mode had interferences at more than one speed, the point at the highest speed would correspond to the highest transmitted torque. Since

excitation torques are often a fixed percentage of transmitted torque, this point would most likely represent the worst case from a stress standpoint. Thus, if all other things were equal, the lower speed points could be dismissed.

Another factor that should be accounted for is the difference in energy levels between the various normal modes. In general, the energy level of a given mode varies inversely with the mode number. Thus, the fundamental mode contains the most energy followed by the second mode, and so on. As a consequence, the lower numbered modes tend to be more responsive to excitations and are more likely to encounter stress problems. Accordingly, with all other variables being equal, if two modes are excited at the same torque level and location, the lower mode will experience higher stresses. This principle can often be used to eliminate higher mode interference points from consideration.

Unfortunately, the above principles cannot be written as hard and fast rules that can be followed for any system encountered, since there are too many variables that must be taken into account. Instead, they are meant to be used as guidelines to be combined with the judgment and experience of the analyst. In many cases, these principles can be used to eliminate most interference points from consideration which greatly reduces the amount of rigorous analysis that must be performed.

The general principles discussed above can be summarized as follows:

- Excitation torques located near nodes have very little impact on the system.
- For a given mode, the worst case point is the one whose pulsating torque location has the highest free vibration amplitude.
- For a given mode, the maximum cyclic torques occur at the locations where the mode shapes have the largest slopes.
- In many machines, the worst case point for a given mode is the one that occurs at the highest speed.
- Interferences with the fundamental and lower numbered modes are usually the most dangerous.

FORCED VIBRATION ANALYSIS

If performance of the preceding steps leaves the analyst with no interference points of concern, the analysis procedure is finished and the system can be declared fully satisfactory. Although this optimum situation will occur occasionally, most times there will still be at least one undismissed interference point remaining. In that case, the next step in the analysis procedure, performance of a forced vibration analysis, should be taken.

In a forced vibration analysis, a known excitation is applied to the system and the resulting vibratory torques and stresses are calculated for each shaft element. Damping due to various sources is included in the model. The induced torques and stresses are then compared to allowable values to determine if the system is structurally adequate.

Excitation Magnitudes

The first step in performing a forced vibration analysis is determination of the magnitudes of the excitations. The various turbomachinery components that can excite machines and their excitation frequencies were discussed in a previous section. In order to determine typical magnitudes for their fluctuating torques, an extensive literature search was undertaken. Unfortunately, with the notable exception of the recent work by Wachel and Szenasi [16], the authors found a dearth of information in this area. Therefore, in many cases, the user should obtain test data from the machine of interest or manufacturer's recommendations in order to determine accurate values.

Wachel and Szenasi [16] recommend the following values for the generic 1× and 2× excitation torques in turbomachinery:

- 1× Excitations: one percent of transmitted torque
- 2× Excitations: 0.5 percent of transmitted torque

The authors cannot claim to have verified the magnitude given for 2× excitations. However, the one percent of transmitted torque figure is in excellent agreement with the authors' experience with turbomachinery. Furthermore, the general trend exhibited, whereas higher order number excitations have lower excitation magnitudes, is in agreement with the literature and the authors' experience. Thus, these recommendations appear to be quite reasonable to the authors.

Gear Excitations

With regards to gear excitations, there are strong disagreements within the literature. Andriola [22], Ehrich [26], and Poritsky [27] all claim that modern gears are cut so accurately that their excitations of torsional vibration are essentially negligible. However, there are at least as many references that cite gear excitations as being the primary cause of observed vibration problems.

The authors believe that it would be unrealistically optimistic to merely disregard gear excitations. Accordingly, the following list of general trends with which the literature is in agreement may be of some assistance to the user:

- The excitation magnitude decreases as the accuracy of the gear improves.
- The excitation magnitude usually decreases as the order number increases.
- Helical gears provide less excitation than do spur gears.
- Spiral bevel gears provide less excitation than do straight bevel gears.
- Fine pitch gears are usually quieter than coarse pitch gears.

As was briefly touched upon earlier, there are two different forms that gear excitations can take. The first type is a torque excitation which is similar to the excitations produced by other components. The sources that can produce the generic 1× and 2× excitations, such as unbalance, misalignment, and ellipticity, are also present in gears. Additionally, the gear contact point can move radially due to tolerances in the tooth profile. All of these sources generate pulsating torques that are applied to the system at the gears.

Additionally, gears can also produce a very different type of 1× excitation known as a displacement excitation. This is also due to errors in the tooth profile, but it is concerned with movement of the contact point in the tangential direction only. This tangential deviation from the nominal position is sometimes referred to as static transmission error. Although this deviation is very small, it can lead to large motions in other portions of the system due to resonance effects.

The mechanism by which tangential errors generate excitations is variation of the gear velocity ratio. The velocity ratio of a pair of mating gears is constant only when motion of the driver produces perfectly smooth rotation of its mate. Such a situation occurs only if both gears are made perfectly. The imperfections that are present in any real pair of gears produce small variations in pitch line velocity which imply that the gears undergo accelerations. These accelerations generate dynamic forces in the gear mesh which can cause the mesh's transmitted load to substantially exceed its steady value.

This increase in maximum transmitted load is often referred to as dynamic loading and is accounted for in most popular gear sizing methods. The variation in force cannot be directly calculated from the gear error since it is strongly dependent on the dynamics of the entire system. Therefore, these excitations must be

input to the model as periodic displacements at the pitch diameter whose amplitudes are equal to the static transmission errors.

Although displacement excitations could theoretically occur at any multiple of gear speed, the higher order excitations could only occur if the static transmission error were distributed symmetrically about the gear's circumference. Since such symmetry is extremely unlikely, the analysis is run using the maximum error at a frequency of once per revolution for each gear in the mesh.

As mentioned before, displacement excitations behave very differently from torque excitations. Specifically, maximum amplification of the tangential error at the gears occurs when the gears are located at a node. In contrast to torque excitations, the further the gears are located away from a node, the smaller is the effect of their displacement excitations.

Ker Wilson [2] explains this apparently anomalous behavior by noting that a shaft performing undamped torsional vibrations is usually considered to be fixed at its nodes. He claims that this is equivalent to placing a disk having infinite inertia at all of the nodes. Applying a fixed displacement excitation to a node is, thus, equivalent to moving an infinite inertia by that same amount. Obviously, the effect of this on the system would be considerable.

Wachel and Szenasi [16] provide the following recommended magnitudes for gear torque excitations:

- 1× Excitations: one percent of transmitted torque
- 2× Excitations: 0.5 percent of transmitted torque

The authors' reaction to these values is the same as that expressed above with respect to the generic 1× and 2× excitations. Unfortunately, Wachel and Szenasi [16] provide no guidelines for excitations at tooth meshing frequency. For these excitations, the authors recommend that a conservative value of one percent of transmitted torque be utilized.

A 1988 seminar [28] provides an alternate method for determining pulsating torque magnitude from the gear's error profile. The first step is to determine, either by test or tolerance study, the radial variation of the gear contact point during one complete revolution of the gear. The excitation torque may then be obtained from the following equation:

$$\tau_{ex} = .5 \bullet \delta_R / R_p \bullet \tau_t \qquad (23)$$

where:

τ_{ex} = Excitation torque
δ_R = Total radial variation in gear contact point
R_p = Gear pitch radius
τ_t = Torque transmitted through gear mesh

As stated above, displacement excitations are input to the model by specifying the tangential component of the gear error.

Before the discussion of gear excitations is concluded, an interesting footnote should be mentioned. In his book, Ker Wilson [2] noted that gears can also generate "phantom" excitations that are determined by the characteristics of the gear-cutting machine and "hereditary" excitations due to the traits of the machine which made the gear-cutting machine. The authors are familiar with an actual case in which these types of excitations caused severe vibration problems in several units of a particular product line. Repeated examinations and inspections could not find any defects in the gears capable of producing the observed vibration. It wasn't until the gear-cutting machine in the vendor's shop was disassembled that the culprit was identified as a slightly defective gear in the machine. Although there isn't much that can be done in the design process to prevent this type of occurrence, knowledge of this phenomenon provides the user with an appreciation for the subtlety of torsional vibration sources.

Impeller Excitations

For pump impeller excitations, Reference [16] gives the following value:

$$\tau_{ex} = 1 / (100 \bullet N_i) \bullet \tau_t \qquad (24)$$

where:

τ_{ex} = Excitation torque
N_i = Number of blades on impeller
τ_t = Transmitted torque

Thus, if Equation (24) is utilized, the excitation torque will be significantly less than one percent of transmitted torque. Heretofore, the authors have never been aware of a correlation between number of impeller blades and excitation torque magnitude, although such a relationship does exist for propellers. Thus, the authors recommend use of the more conservative rule of Artilles, et al. [29], which is to use one percent of transmitted torque for all impellers.

Propeller Excitations

The literature is filled with disagreement on the subject of excitations provided by propellers. In his classic book, Den Hartog [23] recommends use of a value of 7.5 percent of transmitted torque. Poritsky [27] echoes this value. Yates [30] provides several values of torque, dependent on the number of blades, which span the range from four to 12 percent of transmitted torque. On the other hand, Ehrich [26] claims that the excitation torque is only about three percent of transmitted torque. Andriola [22] seems to synopsize the above authors by claiming that the fluctuating torque may vary all the way from two to 15 percent of average torque, depending on number of blades and application. As always, the best approach is to obtain test data for the unit in question, but, in the absence of such, its probably best to conservatively use the maximum value of 15 percent.

Electrical Machine Excitations

The excitations produced by electric motors and generators can be divided into several categories. The first category is normal running at operating speed. For this condition, Wachel and Szenasi [16] recommend the following values for AC motors:

Excitations at line frequency:	one percent of transmitted torque
Excitations at twice line frequency:	0.5 percent of transmitted torque

These values are in general agreement with the authors' experience and are recommended for use with AC generators also.

As was stated previously, the torque pulsations generated during steady running of DC motors and generators are often negligible. Unless the manufacturer says differently, these excitations can normally be ignored.

The second category is the electrical short circuit. As stated previously, when AC motors experience short circuits, they develop torque pulsations at line and twice line frequency. When motors experience large pulsating torques, as is the case during short circuits, the peak torque is often expressed in the peculiar units of "per unit" (pu). This is a shorthand method of expressing the ratio of peak torque to the motor's rated torque. For instance, if a short circuit caused a peak torque that was five times the motor's rated torque, its magnitude would be specified as 5.0 pu. Accordingly, per Pollard [31], typical magnitudes of short circuit torques are as follows:

Excitations at line frequency:	7.0 pu
Excitations at twice line frequency:	3.5 pu

Wolff and Molnar [32] report that these torques may be even higher, claiming levels of 10.0 pu for line frequency excitations and 5.0 pu for those at twice line frequency. Grgic, et al. [33], claim that the excitation torques generated by shorts are significantly reduced if a variable frequency drive is in operation when the short occurs. Unfortunately, they do not specify a numerical value for this attenuation. As is the case with everything else discussed herein, the best source of accurate information is the electrical machine's manufacturer.

The third category is the large transient torques at line frequency that occur instantaneously upon powering of AC motors. Wolff and Molnar [32] claim that the peak torque generated by induction motors can range from 3.0 to 10.0 pu. Pollard [31] estimates that the corresponding peak torques in synchronous motors are about 7.0 to 8.0 pu.

The fourth category is the starting of AC synchronous motors. Since these must be evaluated using a transient analysis, the torque *vs* speed characteristics, for both average and pulsating torques, should be obtained from the manufacturer. Many authors have observed that the maximum pulsating torque during starting can be as high as the motor's rated torque.

Variable Frequency Drive Excitations

The pulsating torques generated by variable frequency AC motor drives are essentially of constant magnitude in the range between 10 and 100 percent of rated speed. As stated before, the magnitudes are much larger between zero and 10 percent of rated speed. Approximate magnitudes are provided in Table 2 for the various harmonics occurring in a six pulse LCI, as taken from Wolff and Molnar [32].

Table 2. Six Pulse LCI Excitation Torques.

Excitation Frequency	Excitation Torque (Percent of Average Torque)	
	(From 0-10% Speed)	(From 10-100% Speed)
6X Electrical Frequency	100	20
12X Electrical Frequency	40	5
18X Electrical Frequency	7	1
24X Electrical Frequency	10	1

Murphy [34] claims that for any VFD, the only excitation that is usually significant is that of the lowest order. Accordingly, for a six pulse drive, the six times frequency excitation is, by far, the most important. The 12, 18, and 24 times frequency excitations are usually small. He proceeds to provide the following representative torque magnitudes for the six times frequency excitation:

Pulse Width Modulator:	5-10 percent of full load torque
Voltage Source Inverter:	10-20 percent of full load torque
Current Source Inverter:	20-30 percent of full load torque

In his nomenclature, full load torque is the maximum torque delivered at a given speed. Even if the actual transmitted torque is somewhat less than this value, he claims that the pulsating torque magnitudes will still obey the above relations.

Sheppard [35] gives torque amplitudes for current source inverters that are identical to those above. On the other hand, Hudson [36] reports of a CSI that produces excitations of only one to two percent of rated torque. Furthermore, the same source that provided the large values listed above, Murphy [34], agrees that special design techniques can be utilized to limit the maximum excitation torques to one or two percent of rated torque.

The torque values presented above are provided merely for the purpose of giving the user a general idea of the magnitudes under consideration. As always, the most accurate numbers for any system can be obtained from the motor manufacturer.

Damping

Once the excitation torques are determined, the next step is identification of all sources of damping in the system. There are two types of damping that can occur in turbomachinery, external and internal. External damping is energy dissipation that is dependent on the absolute velocity of a particular inertia. This kind of damping is modelled as a dashpot between the cognizant inertia and ground. Examples of external damping include damping at impellers and motors.

On the other hand, internal damping is dependent on the difference in angular velocities between two adjacent inertias. Whereas external damping is associated with a particular disk element, internal damping is associated with a specific shaft element. Internal damping is modelled as a dashpot in parallel with the torsional spring representing the appropriate shaft element. Shaft material hysteresis and damping in couplings are modelled as internal dampers.

Both external and internal damping elements are modelled as linear dashpots, as is illustrated in Figure 18.

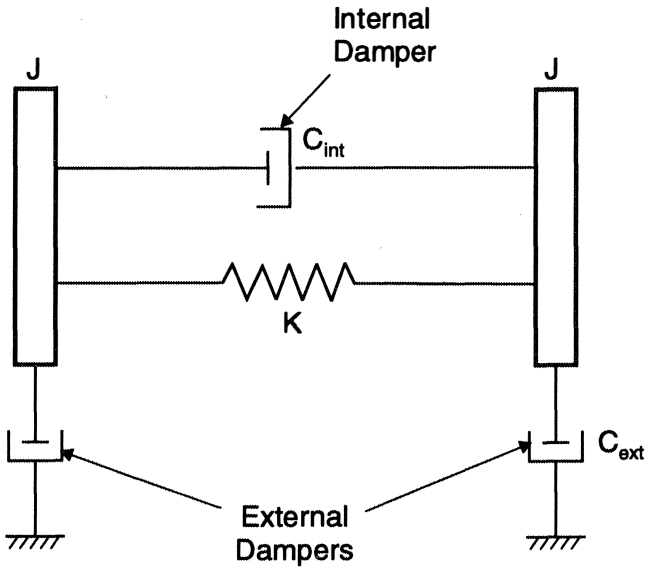

Figure 18. Modelling of Damping.

The torques generated by each oppose the angular velocity and are given by the following equations:

$$\tau_{ext} = c_{ext} \bullet \omega \tag{25}$$

$$\tau_{int} = c_{int} \bullet (\omega_2 - \omega_1) \tag{26}$$

where:

τ_{ext} = Torque generated by external damper (in−lbf)
τ_{int} = Torque generated by internal damper (in−lbf)
c_{ext} = Damping coefficient of external damper (in−lbf−sec/rad)
c_{int} = Damping coefficient of internal damper (in−lbf−sec/rad)
ω = Angular velocity (rad/sec)

There are two common means for specifying the magnitude of damping provided by a specified source. The first and most

straightforward is through use of the damping coefficient used in the above equations. When this method is used, the damping is the same for all vibration modes.

On the other hand, damping is also commonly specified via the damping ratio which is defined as follows:

$$\Gamma = c / c_{cr} \tag{27}$$

where:
Γ = Damping ratio
c = Damping coefficient (in−lbf−sec/rad)
c_{cr} = Critical damping coefficient (in−lbf−sec/rad)

The critical damping coefficient is the lowest value of damping that will prevent oscillations when the system is initially displaced, released, and allowed to freely vibrate until it comes to rest. It is, thus, analogous to the well-known critical damping coefficient for the simple mass-spring system. However, for multiple degree of freedom systems, the critical damping value is not constant, but, rather, is dependent on the vibration mode being considered. The defining equation is as follows:

$$c_{crn} = 2 \bullet \omega_n \bullet J_n \tag{28}$$

where:
c_{crn} = Critical damping coefficient for nth mode (in−lbf−sec/rad)
ω_n = Natural frequency for nth mode (rad/sec)
J_n = Effective inertia for nth mode (in−lbf−sec^2)

The effective modal inertia, J_n, is a weighted summation of the inertias of the individual disks. The procedure for calculating it is provided by Eshleman [3]. It is, therefore, seen that any damping element defined by a damping ratio will have a variable damping coefficient that is dependent on the vibration mode under consideration.

Before the various sources of torsional vibration damping are discussed, it should be pointed out that coulomb friction, which is independent of angular velocity, does not provide damping of torsional vibration. At first, this seems counter to intuition, since one tends to picture a simple torsional spring-mass system where the system is twisted and then released. Such a system would perform free vibrations indefinitely in the absence of friction. If a coulomb friction source were added to the system, energy would be dissipated as heat and the system would eventually come to rest. In this case, damping has unquestionably taken place.

However, the above model is an oversimplification of a turbomachinery drive, since the latter is running at some average speed when torsional vibration is initiated. Since the machine is already rotating prior to excitation, the driver must be providing sufficient torque to overcome any coulomb friction that exists in the system. When torsional vibrations commence, resulting in variations in angular velocity, the coulomb friction's magnitude remains unchanged since it is independent of velocity. The drive torque and coulomb friction torque remain perfectly in balance, regardless of the amplitude of vibration. Unlike the above simplified case, the coulomb friction continuously acts in one direction. It, therefore, theoretically does absolutely nothing to resist the vibration and is, thus, not a damping element.

Load Damping

One of the primary sources of damping in turbomachinery systems is the torque *vs* speed characteristic of the load. This applies regardless of whether the load is an impeller, electric generator, or propeller. If the load is such that its resisting torque increases as speed is increased, with all other parameters held constant, then it is a source of damping. Furthermore, the viscous damping coefficient is equal to the instantaneous value of the slope of the torque *vs* speed curve at the operating point.

The reason such a characteristic results in damping requires some elaboration. As stated previously, torsional vibration results in instantaneous speed fluctuations about the average machine speed. If a component has a positive torque *vs* speed characteristic, then during the portion of the vibration cycle when the speed is above the mean value, the resisting torque increases. The additional resisting torque attempts to slow the system down and, thus, opposes the vibratory motion.

On the other hand, during the time when the speed is below the steady state value, the resisting torque goes down. This reduction in opposing torque tends to accelerate the system and, thereby, also opposes the torsional vibration. Therefore, the torque-speed characteristic of the load tends to oppose the vibration throughout its entire cycle and, thus, acts as a source of damping.

Of course, this phenomenon is dissipative only if the slope of the torque *vs* speed characteristic is positive. If the slope were negative, the situation would be exactly the opposite of that discussed above and the load would act to enhance the vibration. In that case, the damping would be negative and instability could result if there weren't other damping sources in the system to suppress the vibration. Fortunately, most practical impellers and propellers provide positive damping over their entire operating ranges. The same cannot be said, however, of generators since their torque *vs* speed curves sometimes exhibit negative slopes at speeds below rated speed.

The above discussion also applies to drivers such as motors and turbines with one major modification. Although the magnitude of the damping coefficient is still equal to the slope of the torque *vs* speed curve, the sign is reversed. That is, in order for the driver to supply positive damping, the slope of its torque-speed curve must be negative. This sign change is necessary because the driver is an energy source rather than an energy absorber.

When generating the torque *vs* speed curve for the purpose of calculating a damping coefficient, it is essential that all other relevant parameters be held constant. This means that the fluid properties and flowrate must be held constant for an impeller, the vessel speed must be constant for a propeller, and the voltage must be held fixed for an electrical device.

Failure to follow the above rule can lead to extremely misleading results. For instance, turbines are often used as drivers in turbomachinery. In such cases, the steady state torque *vs* speed curve for the turbine usually has a positive slope, reflecting the higher power generated at high speeds. The reason the turbine produces more torque at higher speed is that the flow rate increases with speed. Thus, if one were to merely take the slope of the steady state curve, the erroneous conclusion that the turbine is a source of negative damping would be arrived at. Thus, it is imperative that the flow rate be held constant during generation of the curve so that the true positive damping characteristic will emerge.

As is the case with generators, some motors are sources of negative damping. This is especially common with AC induction and synchronous motors that often have a positive torque *vs* speed characteristic over a large portion of the speed range below synchronous speed.

Although the torque-speed curve method just described is the most accurate method for obtaining damping coefficients for load and driver elements, there are other approximate equations provided in the literature. For instance, Nestorides [8] provides a detailed method for calculating the damping factor for propellers as a function of their dimensions. Additionally, many authors approximate the torque-speed relation for a propeller by the following:

$$\tau_{prop} = k \bullet \omega_{prop}^{\,n} \tag{29}$$

where:
τ_{prop} = Propeller torque (in−lbf)

k = Constant
ω_{prop} = Propeller angular velocity (rad/sec)
n = Propeller exponent

Most authors give the value of n as being between two and three. By differentiation with respect to ω_{prop}, the damping coefficient is then given by the following:

$$c_{prop} = n \bullet k \bullet \omega_{prop}^{(n-1)} \quad (30)$$

where:
c_{prop} = Propeller damping coefficient (in−lbf−sec/rad)

For approximation purposes, Ker Wilson [2] claims that most propellers yield damping coefficients that are between five and 10 percent of critical damping.

The damping from turbomachinery impellers is usually much smaller than that arising in propellers. Yates [30] claims that turbines provide damping that is between 0.15 and 0.50 percent of the critical value. Smalley [37] claims a typical value for compressor rotors is 0.2 percent of critical. In many practical impellers, the torque is approximately proportional to the square of the speed. Therefore, Equations (29) and (30) can be used with a value of two for n to estimate the damping coefficient if at least one torque speed point is known.

Nestorides [8] provides the following equation for estimating the damping coefficient of a DC generator:

$$c_{gen} = 600{,}000 \bullet V / (V - V_c) \bullet hp / RPM^2 \quad (31)$$

where:
c_{gen} = DC generator damping coefficient (in−lbf−sec/rad)
V = Total generator voltage (terminal voltage plus internal drop) (Volts)
V_c = Counter EMF of driven machinery (motor or storage battery but not an external resistance) (Volts)
hp = Generator power (hp)
RPM = Shaft speed (rpm)

Ker Wilson [2] states that the above equation is also applicable to DC motors.

Both Ker Wilson [2] and Nestorides [8] state that the damping in standard AC motors and generators is negligible. It is common, therefore, to equip these machines with damper windings. When this is done, the damping coefficient can be approximated using Equation (31). Ker Wilson [2] claims that generators with damper windings can achieve damping as high as 25 percent of the critical value.

Windage Damping

Another source of external damping is the windage frictional loss that occurs due to viscous fluid drag on immersed impellers. Windage friction generates damping, unlike coulomb friction, since the frictional force generally increases with speed. This damping is usually negligible for impellers surrounded by air such as compressor and turbine rotors. However, pump impellers immersed in a highly viscous liquid can generate damping torques that are not insignificant. Ker Wilson [2] provides the following equation for the torque due to friction acting on all surfaces of a hollow disk:

$$\tau_V = \pi \bullet \mu \bullet \omega \bullet (R_o^3 \bullet (R_o + 2L) - R_i^4) / h \quad (32)$$

where:
τ_V = Frictional torque (in−lbf)
μ = Fluid absolute viscosity (lbf−sec/in^2)
ω = Disk angular velocity (rad/sec)
R_o = Disk outside radius (in)
R_i = Disk inside radius (in)
h = Radial clearance or axial clearance (assumed equal) (in)
L = Disk length (in)

Differentiation of the above with respect to angular velocity yields the following equation for damping coefficient:

$$c_v = \pi \bullet \mu \bullet (Ro^3 \bullet (Ro + 2L) - Ri^4) / h \quad (33)$$

where:
c_v = Damping coefficient (in−lbf−sec/rad)

Journal Bearing Damping

Another damping source is the fluid-film journal bearing. The viscous friction that occurs in these bearings is speed-dependent and is, therefore, theoretically a provider of damping. However, many authors note that the damping due to viscous friction in bearings is virtually negligible. The interested reader can demonstrate this by merely differentiating the classical journal bearing friction equation with respect to angular speed and calculating the resulting damping coefficient.

However, journal bearings can be significant, even dominant, sources of damping if any lateral motion accompanies the torsional vibration. Lateral motion can arise if there is a coupling between torsional and lateral modes. Such coupling is very common in geared systems due to the radial load at the gear mesh. When the journal moves laterally, it forces the fluid in the radial clearance to flow circumferentially, generating a squeeze film effect. Simmons and Smalley [6], Draminsky [38], and Shannon [39] all report of cases where this squeeze film action was the preeminent source of damping in the system. Furthermore, Smalley [37] claims that this mechanism can yield damping ratios as high as 0.10.

Although this mechanism can be highly significant, especially in geared systems, its magnitude is very difficult to calculate. Per Smalley [37], in order to determine the damping coefficient, a combined torsional-lateral model of the gear mesh needs to be created and executed. Since such an undertaking is often complicated and time consuming, it does not always represent a practical alternative. Accordingly, the authors recommend that journal bearing damping be completely ignored in ungeared systems. In geared systems, the beneficial aspects of squeeze film action can be accounted for by judiciously increasing the system's modal damping ratio, to be discussed later on.

Shaft Hysteretic Damping

All of the damping sources discussed up to now qualify as external damping phenomena. Accordingly, their damping is associated with a specific disk element. The remaining damping sources to be described are internal damping mechanisms which are linked to shaft elements.

Material hysteresis is the dissipation of energy that occurs when a metal is subjected to a complete cycle of stress changes within its elastic region. Energy is dissipated because all real metals slightly deviate from idealized Hooke's law behavior due to plastic deformations at the microscopic level. These cause the material's behavior during unloading to be slightly different than it was during loading. An exaggerated depiction is shown in Figure 19 of the stress-strain behavior of a real material taken through a complete stress cycle. It is seen from the figure that the strain slightly lags behind the stress such that there is a finite residual strain in the material when all stress is removed.

The implication of this is that when a shaft is twisted in either direction and then released, it does not return to its initial position

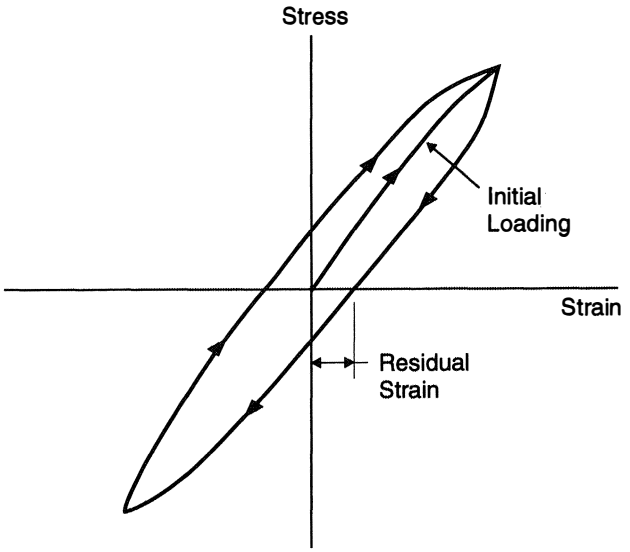

Figure 19. Material Hysteresis Loop.

of zero deflection. In order to bring the shaft back to the unstrained position, a finite amount of work must be added to the system. This work is needed to make up for the hysteresis energy dissipated during twisting and releasing of the shaft. This energy loss is due to internal friction within the material and is released in the form of heat. If a material is taken through a complete stress cycle, the total energy dissipation is equal to the area enclosed in the stress-strain loop.

There has been a plethora of technical articles written on the subject of material hysteresis. Some general characteristics of this phenomenon are as follows:

- The energy lost due to hysteresis during cycling is a very small fraction of the elastic energy at the maximum stress point.
- Energy loss is essentially independent of frequency of cycling.
- The energy dissipated per cycle is strongly dependent on the cyclic stress level in the material. Dissipation and damping increase as stress increases.
- Above a certain stress level, known as the quasicritical stress, the relationship between applied stress and hysteresis loss changes dramatically. Above this point, relatively small stress level increases result in large increases in energy dissipation.
- Hysteresis, as specified by the energy lost per cycle per unit volume, is a material property. It is totally independent of part size and form.
- The hysteresis exhibited by a given material at a specified stress level is a function of the material's stress history. Parts that have previously been taken above the quasicritical stress level will exhibit significantly larger damping at the same stress level than those that have never crossed this threshold.
- In general, configurations where most of the material is at a high stress level provide higher levels of damping. Thus, for a given torsional stress level, a hollow shaft provides more damping than a solid shaft having the same volume since a greater portion of the material is in the vicinity of the highly-stressed outer surface.

In general, the relationship between energy dissipation and cyclic stress level can be expressed by the following equation:

$$D = A \cdot \sigma^m \quad (34)$$

where:
D = Specific energy loss (in−lbf/cycle/in^3)
A = Material constant
σ = Amplitude of cyclic shear stress (psi)
m = Hysteresis exponent

Accordingly, the cyclic energy loss in a hollow circular shaft that obeys the relation of Equation (34) is as follows:

$$E = A \cdot 2\pi / (2 + m) \cdot (R_o^{(m+2)} - R_i^{(m+2)}) / R_o^m \cdot \sigma^m \cdot L \quad (35)$$

where:
E = Energy loss per cycle (in−lbf/cycle)
R_o = Outside radius (in)
R_i = Inside radius (in)
L = Length (in)

At stresses below the quasicritical limit, most authors agree that the hysteresis exponent is between two and three. An exponent espoused by several authors for steel is 2.3. Above the quasicritical stress, the exponent increases dramatically and can reach values as high as 10.5, according to Dorey [40]. Dorey [40] also found experimentally that the quasi-critical stress for steel is between 12,000 and 30,000 psi. Several sources note that this limit can be approximated by dividing the material's ultimate tensile strength by five.

Unfortunately, Equation (35) does not lend itself easily to forced vibration analysis. To facilitate calculation, shaft hysteresis is usually modeled as a viscous internal damping element. The assumption of viscous damping implies a value of 2.0 for the hysteresis exponent so it is relatively accurate for shafts at low stress levels. However, the error introduced is considerable for highly-stressed shafts.

The equivalent viscous damping coefficient can be calculated for a given mode of vibration by using the following:

$$c_{eq} = D \cdot VOL / (\pi \cdot \omega_n \cdot \theta_{sh}^2) \quad (36)$$

where:
c_{eq} = Damping coefficient (in−lbf−sec/rad)
D = Specific energy loss (in−lbf/cycle/in^3)
VOL = Volume of material in shaft (in^3)
ω_n = Natural frequency (Rad/sec)
θ_{sh} = Angle of twist in shaft (rad)

Unfortunately, the damping coefficient is seen to be dependent on the amplitude of vibration which is usually the unknown quantity. An iterative solution is needed, therefore, if Equation (36) is to be utilized. This is far from a trivial task and is not the method preferred by the authors.

Instead, like the majority of sources consulted, the authors recommend use of a representative damping ratio which is applied to all shaft elements in the model. The literature is filled with various recommendations for the magnitude of this ratio. Ehrich [26] specifies a value of 0.16 percent of critical for typical rotor steels. Draminsky [38] essentially agrees, citing a value of 0.2 percent. Ker Wilson [2] claims typical factors of 0.2 to 0.4 percent of critical. Rieger [41] claims that the damping is closer to 0.5 percent. Finally, a 1988 seminar [28] recommended use of 0.5 to 1.0 percent.

No matter which of the above values is selected, it is readily apparent that the hysteretic damping is relatively small. Because of this, the authors recommend lumping the hysteresis damping with several other indeterminate damping sources to be discussed shortly in one overall empirical damping ratio.

Another source of internal damping is couplings containing rubber elements. The mechanism by which these dissipate energy is exactly the same as that just discussed for steel shafts. The major difference is that rubber generates an order of magnitude more hys-

teresis than do metals. Rubber couplings can generate damping as high as 25 to 30 percent of critical [28]. Of course, the best source for accurate damping data is the coupling manufacturer.

Hydraulic Coupling Damping

Another type of coupling that can provide substantial damping is the hydraulic coupling that was described earlier. As was pointed out, this coupling has the beneficial aspect of effectively dividing a torsional system into two independent systems. This permits the isolation of vulnerable components from significant sources of vibration such as synchronous motors.

In addition to its isolation characteristic, the fluid coupling also provides damping to the machine by virtue of viscous friction between the impellers and coupling fluid. Per Ker Wilson [2], although this damping can be significant, it is usually considerably less than that of a marine propeller at the same power level. He proceeds to then provide the following equation for a coupling operating with lube oil at three percent slip:

$$c = 600{,}000 \bullet (1 + 1 / n^2) \bullet hp / RPM^2 \qquad (37)$$

where:
c = Damping coefficient (in−lbf−sec/rad)
n = Order number of mode being excited
hp = Average power transmitted through coupling (hp)
RPM = Speed of driving shaft (rpm)

This equation is also independently given by Nestorides [8]. It should be noted that the above equation should only be used for approximate ballpark numbers, since damping is a function of fluid type, operating temperature, and slip that are not accounted for in this equation. For accurate damping values, the coupling manufacturer should be consulted.

Speed Variation Damping

A source of damping that is not provided by a specific component is apparent damping due to speed variations. This source is not an energy dissipation mechanism per se; rather, it represents the fact that speed variation can occur in real machines, resulting in imperfect resonance. If the running speed is assumed to vary in a periodic manner, Nestorides [8] gives the following formula for the effective increase of all damping coefficients in the system:

$$c = c_o / \cos(B \bullet R / \pi) \qquad (38)$$

where:
c = Apparent damping coefficient (in−lbf−sec/rad)
c_o = Damping coefficient calculated in normal manner
R = Number of torsional vibration cycles that occur in one speed variation cycle

The coefficient B is obtained from the following:

$$B = (RPM_{max} - RPM_{min}) / RPM_{mean} \qquad (39)$$

where:
RPM_{max} = Maximum machine speed (rpm)
RPM_{min} = Minimum machine speed (rpm)
RPM_{mean} = Average machine speed (rpm)

In most practical systems, speed variation damping is small and can often be neglected.

Slip Damping

Another important source of damping in torsional systems is slip damping. Slip damping arises from friction between two surfaces which are brought into relative motion by the vibration. Locations where this commonly occurs include bolted flanged joints, splines, keyed connections, and shrink fits. It should be noted that this mechanism is very different from the coulomb friction described previously since there is no relative motion or friction prior to the onset of vibration.

Unfortunately, there are no practical methods for calculating the magnitude of slip damping. However, it appears that it plays a major role in many real systems. Many authors have observed that the damping occurring in practice is almost always significantly greater than the calculated value. Many attribute this discrepancy to the presence of slip damping.

Because of the difficulty in calculating hysteresis and slip damping, many experts advocate lumping the two together in an empirical damping ratio that is applied to every shaft element in the model. This is the method recommended by the authors. All other sources of damping such as impellers, motors, and journal bearings should be simultaneously included in the model.

There is a considerable difference of opinion in the literature regarding the percentage of critical damping that should be assumed. A representative sample of recommended values is provided in Table 3. Unfortunately, the tabulated numbers are somewhat nebulous, since the majority of the sources neglect to specify whether a geared or ungeared configuration is under consideration. The authors have found through experience that assuming damping of one percent of critical is conservative for ungeared systems.

Table 3. Recommended Damping Ratios [42, 43, 44, 45, 46].

Source	Damping Ratio (Γ)
Enrich [26]	0.004
Grgic, et al. [33]	0.005
Frei, et al. [42]	0.01
McCann and Bennett [12]	0.005 - 0.020
Thames and Heard [43]	0.0083 - 0.025
Evans, et al. [44]	0.0167
Vance [1]	0.015 - 0.020
Wachel and Szenasi [16]	0.0167 - 0.025
Ker Wilson [2]	0.025
Yates [30]	0.025
Chen [45]	0.01 - 0.05
Reference [28]	0.01 - 0.05
Artilles, et al. [29]	0.01 - 0.05
Simmons and Smalley [6]	0.01 - 0.06
Chen, et al. [46]	0.03 - 0.05

There is little doubt that the damping in geared systems is generally higher than for ungeared ones due to the squeeze film effect in fluid-film journal bearings. Ker Wilson [2] goes so far as to claim that the damping is doubled. Wright [47] is more cautious, claiming that the damping ratio increases from 0.0125 to 0.020. Unfortunately, there are few other recommendations regarding the amount by which damping should be increased when dealing with a geared system. It seems safe, however, to moderately increase the empirical factor used for ungeared assemblies if there are fluid-film bearings present.

Steady State Analysis

Once the excitation torques and damping coefficients are determined, the steady state forced damped analysis can be performed. In general, a separate analysis should be performed for each interference point remaining under consideration. As was the case with the undamped analysis, the mechanics of setting up and solving the relevant equations are not of prime importance since there are many good computer codes available for doing this. Once again, the primary emphasis is placed on generation of the correct input values and proper utilization of the analysis results.

Forced torsional vibration occurs when a sinusoidal excitation is applied to a machine operating at a constant speed, N. The system response is obtained by solving the differential equations of motion. In general, the solution is known to consist of two components, the complimentary solution and the particular solution. The complimentary solution is a transient free vibration at the natural frequency that decays to zero exponentially with time. Yates [30] asserts that the complimentary response typically takes about 20 vibration cycles to die out. Conversely, the particular solution is a steady state term that continues for as long as the excitation is applied. In steady state analysis, the particular solution is the only term of interest.

For any system, the particular solution consists of a continuous oscillation at the excitation frequency, ω. This oscillation is superimposed on the steady running speed, N. The net result is that the disks no longer rotate at a constant speed. Instead, their angular velocity varies sinusoidally between the limits of $N-\omega$ and $N+\omega$, assuming N and ω are in consistent units.

Unlike the undamped case, the disks do not vibrate in phase with each other during forced vibration. The system's damping introduces phase shifts to all disks such that their individual motions are given by the following equation:

$$\theta = \theta_o \cdot \sin(\omega t - \phi) \tag{40}$$

where:
θ = Angular position of a given disk as a function of time
θ_o = Amplitude of angular vibration
ω = Angular frequency (rad/sec)
t = Time (sec)
ϕ = Phase angle between displacement and excitation (rad)

The lumped model used for the damped analysis is essentially the same as that utilized for the undamped calculation. The only difference is that internal and external damping elements must be added in the appropriate locations. In torsional systems, as in other vibrating systems, damping has a significant impact on the response only at frequencies near resonance. However, since the only forced vibration analyses that will be discussed herein are concerned with the resonant condition, damping shall always be included.

In the analysis to be discussed, torque and/or displacement excitations are applied to the system at appropriate locations. Since they are applied at a resonant frequency, the response would be infinite if there were no damping in the system. However, since damping is present, the response builds up until the total energy input to the system by the various excitation sources equals the total energy dissipated by the dampers. At this point, the system begins steady state vibration.

Geared Systems

Geared systems are handled in the same manner as in the undamped analysis. All inertias and spring rates are converted to equivalent values at the lowest speed shaft via Equations (4) and (5). Both internal and external damping elements located on the high speed shaft are converted to equivalent values in the same manner, as illustrated in the following:

$$c_{eq} = c \cdot N^2 \tag{41}$$

where:
c_{eq} = Equivalent damping coefficient referenced to low speed shaft
c = Actual damping coefficient
N = Gear ratio (N > 1.0)

However, when equivalent systems are used, the displacements and torques occurring in the equivalent elements have no physical meaning. In order to determine the displacements and torques occurring in the actual physical shafts, the procedure for generating the equivalent system must be reversed. That is, the equivalent displacements and torques at the lowest speed shaft must be converted through all of the appropriate gear meshes until the desired shaft is reached. The conversion equations for any gear mesh are as follows:

$$\theta = \theta_{eq} \cdot N \tag{42}$$

$$\tau = \tau_{eq} / N \tag{43}$$

where:
θ = Angular displacement at high speed shaft
θ_{eq} = Equivalent angular displacement at low speed shaft
N = Gear ratio (N > 1.0)
τ = Torque at high speed shaft
τ_{eq} = Equivalent torque at low speed shaft

Nonlinear Couplings

As was the case in the undamped analysis, nonlinear couplings demand special attention during the performance of a forced vibration analysis. Tuplin [48] advocates use of an equivalent linear spring that would contain the same amount of strain energy as the actual coupling when subjected to a specified angle of twist. Since the strain energy accumulated by a nonlinear coupling is equal to the area under the torque *vs* angle of twist curve (Figure 6) up to the specified twist angle, θ_t, the equivalent stiffness can be calculated from the following:

$$k_{eq} = 2 \cdot A / \theta_t^2 \tag{44}$$

where:
k_{eq} = Spring rate of equivalent linear element (in−lbf/rad)
θ_t = Angle of twist in coupling (rad)
A = Total area under τ *vs* θ curve up to θ_t

It is seen that the equivalent stiffness is a function of the angle of twist which is an unknown. Accordingly, as was done in the undamped analysis, an iterative procedure must be implemented. The steps to be taken are as follows:

- Assume an angle of twist, θ_t, in the coupling.
- Calculate the equivalent spring rate using Equation (44).
- Using this stiffness, perform the forced vibration analysis and determine the actual twist in the coupling.
- If the actual twist in the coupling matches the assumed value, a solution has been found. If not, go back to step 1 and try another guess value.

Since each interference point will most likely induce a different amount of twist in the coupling, the above procedure should be repeated for each point analyzed.

Electrical Machines

The reader may find the various combinations of electrical machine types and drives to be somewhat confusing. To alleviate

any confusion, the various cases that should be investigated for different motor-drive combinations are listed in Table 4. The cases tabulated as steady state can be analyzed using the procedures to be discussed next. The transient cases will be addressed in a later section. It should be emphasized that only those cases whose excitation line generates an interference point need to be analyzed. Thus, for many systems, many of the listed cases will not require analysis.

Table 4. Relevant Cases for Various Electrical Machines.

Machine Type	Drive Type	Case	Excitation Frequencies	Steady State or Transient
AC Generator with N_p Poles		1. Steady Running	Line Frequency	Steady State
		2. Steady Running	2 x Line Frequency	Steady State
		3. Steady Running	N_p x RPM	Steady State
		4. Short Circuit	Line Frequency	Transient
		5. Short Circuit	2 x Line Frequency	Transient
AC Motor with N_p Poles	Fixed Frequency	1. Steady Running	Line Frequency	Steady State
		2. Steady Running	2 x Line Frequency	Steady State
		3. Steady Running	N_p x RPM	Steady State
		4. Short Circuit	Line Frequency	Transient
		5. Short Circuit	2 x Line Frequency	Transient
		6. Initial Start	Line Frequency	Transient
		7. Runup to Speed (synchronous only)	2 x Slip Frequency	Transient
AC Motor with N_p Poles	Variable Frequency with N Pulses (except Static Kramer)	1. Steady Running	$^1/_2$ x N_p x RPM	Steady State
		2. Steady Running	N_p x RPM	Steady State
		3. Steady Running	$^1/_2$ x N x N_p x RPM	Steady State
		4. Steady Running	N x N_p x RPM	Steady State
		5. Steady Running	1.5 x N x N_p x RPM	Steady State
		6. Steady Running	2 x N x N_p x RPM	Steady State
		7. Short Circuit	$^1/_2$ x N_p x RPM	Transient
		8. Short Circuit	N_p x RPM	Transient
		9. Initial Start (induction only)	Line Frequency	Transient
AC Motor with N_p Poles	Static Kramer Drive with N Pulses	1. Steady Running	Line Frequency	Steady State
		2. Steady Running	2 x Line Frequency	Steady State
		3. Steady Running	N_p x RPM	Steady State
		4. Steady Running	N x Slip Frequency	Steady State
		5. Steady Running	2N x Slip Frequency	Steady State
		6. Short Circuit	Line Frequency	Transient
		7. Short Circuit	2 x Line Frequency	Transient
		8. Initial Start	Line Frequency	Transient

Analysis Methods

There are many different methods that can be employed to solve steady state forced torsional vibration problems. A few of them will be briefly discussed to give the user a flavor for the type of techniques commonly utilized. However, as is the case with undamped analysis, the authors do not believe that the mechanics of the solution procedures are of primary importance, since there are many computer codes available to the user. Accordingly, descriptions of the various methods are kept brief.

Energy Balance Method

Perhaps the simplest method for steady state resonant forced vibration analysis is that which Ehrich [26] refers to as the energy balance method. The basis for this procedure is that, at steady state, the amount of energy input to the system by the excitation torques during a vibration cycle must be equal to that dissipated by the damping elements. The key assumption utilized in this method is that the damping level is so light that it has no impact on the system's natural frequency and mode shape. The assembly is, therefore, assumed to execute forced vibration at its undamped natural frequency with its undamped mode shape. Implementing this assumption, the energy input by each excitation is:

$$E_i = \pi \bullet \tau_{exc} \bullet \theta \tag{45}$$

where:
E_i = Energy input per cycle by excitation source (in−lbf)
τ_{exc} = Excitation torque (in−lbf)
θ = Angular displacement at excitation location (rad)

Likewise, the energies dissipated per cycle in external and internal dampers, respectively, are given by the following:

$$E_{de} = \pi \bullet w_n \bullet c_{ext} \bullet \theta^2 \tag{46}$$

$$E_{di} = \pi \bullet w_n \bullet c_{int} \bullet (\theta_2 - \theta_1)^2 \tag{47}$$

where:
E_d = Energy dissipated per cycle by damper (in−lbf)
ω_n = Natural frequency (rad/sec)
c = Damping coefficient (in−lbf−sec/rad)
θ = Angular displacement at damper location (rad)

In the above equations, the unknown parameters are the angular displacements. However, the ratios of the various displacements are fixed by the mode shape. Combining these ratios with the above equations, the steady state amplitudes at each disk can be solved for.

Complex Holzer Method

The preceding method is reasonably accurate for most torsional systems, since they are usually lightly damped. However, it is not appropriate for systems that contain a large damping element such as a hydraulic coupling. To permit analysis of such systems, Den Hartog and Li [49] propose a method that utilizes a variation of the Holzer table. Although their method is more complicated than the energy balance method, it does not suffer from any of its limiting assumptions.

In the Den Hartog/Li procedure [49], a Holzer table containing complex quantities is generated. The real part of each quantity represents the portion that is in phase with the motion of the shaft's first disk while the imaginary part is 90 degrees out of phase with that motion. As with Holzer's method of finding undamped natural frequencies, this method requires generation of a table for each guessed value of the vibration frequency. The remainder torque is determined for the last disk for various frequencies until the frequency which yields the minimum remainder torque is found. This frequency is the damped natural frequency which for most torsional systems is not much different from the undamped value.

The damped natural frequency is found by setting the amplitude at the first disk arbitrarily to one radian. The amplitudes at the various disks in the table for the damped natural frequency represent the mode shape of damped vibration. After determination of the natural frequency, this Holzer table is manipulated further until the appropriate disk torques are equal to the excitation torques. The resulting displacements are then the actual forced vibration amplitudes of the system.

Modal Analysis

Modal analysis is a relatively simple, approximate method for determining the induced torques in a system undergoing forced vibration. Artilles, et al. [29], provide an equation for the angular displacement at a given disk as a function of the excitation torques applied at other disks. The equation consists of a weighted summation of all of the mode shapes of the system, which is technically an infinite number. However, Artilles, et al. [29], claim that relatively accurate results can be obtained using only the first four or five mode shapes.

The modal analysis method is not exact because it assumes that the damping in the system is small. However, this is a good assumption for the majority of torsional systems encountered in practice. Additionally, this procedure suffers from the limitation

that the only damping input is a modal damping ratio which is applied to all shaft elements. Thus, individual damping sources located at specific positions cannot be incorporated in the model. However, since many torsional analyses are conducted with an empirical damping ratio as the only damping input, this is not as much of a restriction as it may first appear to be. Vance [1], Eshleman [3], and Poritsky [27] all provide more detailed descriptions of this analysis procedure.

Matrix-Eigenvalue Methods

Matrix-eigenvalue methods, which were previously described for the natural frequency analysis, can also be used for forced vibration calculations. The matrix equation for forced vibration is an extension of Equation (10) and is as follows:

$$[k] \bullet [\theta] + [c] \bullet [\omega] + [J] \bullet [\alpha] = [\tau] \qquad (48)$$

where:
[k] = Stiffness matrix
[c] = Damping matrix
[J] = Inertia matrix
[τ] = Excitation torque vector
[θ] = Angular displacement vector
[ω] = Angular velocity vector
[α] = Angular acceleration vector

The stiffness and inertia matrices are the same as those used in the undamped analysis. The damping matrix is a combination of the damping coefficients of all of the external and internal dashpots in the system. Vance [1] provides specifics for generating each of these matrices.

As in the undamped analysis, matrix methods are used to determine the eigenvalues and eigenvectors. Due to the inclusion of damping, these are all complex. The damped natural frequencies are equal to the square roots of the imaginary portions of the eigenvalues. The displacements of the individual disks are obtained from the eigenvectors.

Shaft Torques and Stresses

All of the forced vibration analysis procedures are designed to obtain the amplitude and phase angle of each disk in the system. Once these are determined, the cyclic torque in each shaft is easily obtained from the following:

$$\tau_{12}(t) = k_{12} \bullet (\theta_1(t) - \theta_2(t)) + c_{12} \bullet (\omega_1(t) - \omega_2(t)) \qquad (49)$$

where:
τ_{12} = Cyclic torque occurring in shaft between disks 1 and 2 (in−lbf)
k_{12} = Spring rate of shaft between disks 1 and 2 (in−lbf/rad)
θ_1 = Angular displacement of disk 1 (rad)
θ_2 = Angular displacement of disk 2 (rad)
c_{12} = Damping coefficient for shaft between disks 1 and 2 (in−lbf−sec/rad)
ω_1 = Angular velocity of disk 1 (rad/sec)
ω_2 = Angular velocity of disk 2 (rad/sec)

Once the cyclic torque acting on a particular shaft is known, the resulting maximum shear stress can be calculated using the following equation from strength of materials:

$$S_s = \tau \bullet R / I_p \qquad (50)$$

where:
S_s = Maximum shear stress in shaft (psi)
τ = Torque acting on shaft (in−lbf)
R = Shaft radius (in)
I_p = Area polar moment of inertia (in^4)

Analysis Methodology

Once the analysis procedure is selected, it should be used to evaluate each remaining interference point, one at a time. Since each interference point is driven by a specific excitation source, there should only be one excitation torque applied to the model. The location of this torque is fixed if it is due to a specific component in the system, such as an impeller or motor. However, if the excitation is a generic one such as the 1× and 2× drivers resulting from unbalance or misalignment, it could be located at literally any disk in the system. In this case, the authors advocate application of the excitation at the disk which exhibits the maximum displacement in the appropriate mode shape. This represents the worst case from an induced torque and stress standpoint and is, therefore, conservative.

Additionally, if any of the interference points arise from displacement excitation at a gear mesh, that case should be analyzed separately. In order to accomplish this, the solution algorithm being used must be flexible enough to accept a displacement input. Badgley and Laskin [50] discuss how to achieve this and provide a sample computer program.

The authors have saved time on many occasions by executing an initial run with the damping due to specific sources ignored. The only damping included is the generic damping ratio of 0.01 applied to each shaft element in the model. As discussed previously, this accounts for hysteretic and slip damping effects and represents the minimum amount of damping that can reasonably be expected. The results obtained from this run are, thus, conservative.

If the results from this initial run are deemed acceptable according to the criteria to be discussed later, then the analysis for that particular interference point is complete. The analyst has saved the often considerable time and effort required to determine the damping coefficients due to the various individual sources. If the results are not acceptable, the analyst then must calculate the appropriate coefficients and rerun with them applied.

Even if the initial run is not successful in validating the design, the analyst need not calculate every single damping coefficient for the more rigorous run. As is the case with excitation torques, damping elements only have a significant impact on the system if they are located in regions of significant vibratory activity, as defined by the cognizant mode shape. This refers to the amplitude at the appropriate disk for an external damper and the angle of twist in the accompanying shaft for an internal dashpot. Thus, when running the analysis, the user can ignore damping elements located in dormant areas of the system.

Analysis Results

The results of a steady state analysis consist of the angle of twist, cyclic torque, and cyclic stress occurring in every shaft element in the model. Additionally, the torques and deflections for each disk element are also often presented. These results should be utilized to determine the adequacy of the system, based on three general criteria.

Shaft Fatigue Stress

The first criterion is the structural integrity of each shaft element. Each shaft is subjected to a combination of mean stress due to the average transmitted torque and cyclic stress due to the torsional vibration. The cyclic stress obtained from the vibration analysis is a nominal value, calculated using Equation (50), based on the macroscopic properties of the shaft cross-section.

The nominal cyclic stress should be increased by appropriate stress concentration factors to account for the presence of keyways, splines, fillet radii, etc. The corrected cyclic stress should then be

plotted along with the mean stress on a Goodman diagram for the shaft material. The equivalent fully-reversing stress can then be obtained by drawing a straight line from the plotted point to the material's ultimate strength in shear. As is illustrated in Figure 20, extension of this line to the y-axis yields the equivalent stress value.

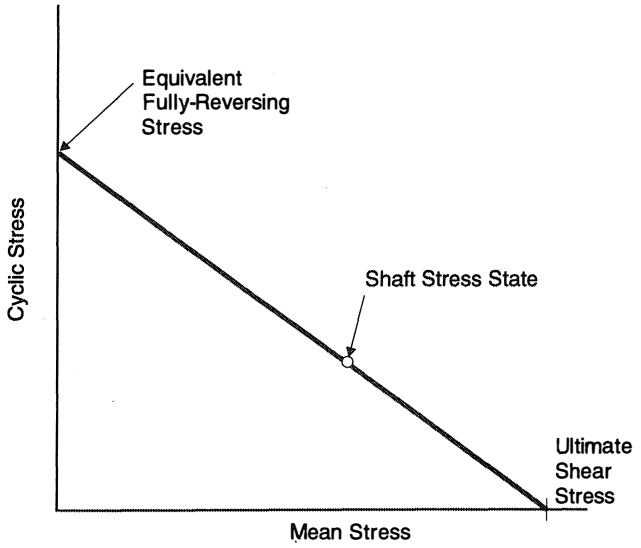

Figure 20. Typical Goodman Diagram.

Alternately, the equivalent fully-reversing stress can also be calculated from the following formula:

$$S_{eq} = S_{ult} / (S_{ult} - S_{mean}) \bullet S_{cyclic} \quad (51)$$

where:
S_{eq} = Equivalent fully-reversing stress
S_{ult} = Material ultimate strength in shear
S_{mean} = Mean stress
S_{cyclic} = Cyclic stress

This equivalent stress should then be compared with the material's endurance limit, corrected for all of the appropriate factors such as size, temperature, and surface finish. The endurance limit must be used since resonance at a normal operating speed can induce a virtually infinite number of stress cycles. The endurance limit and equivalent stress should then be combined to determine the safety factor as follows:

$$SF = S_e / S_{eq} \quad (52)$$

where:
SF = Safety factor
S_e = Endurance limit (psi)
S_{eq} = Equivalent fully-reversing stress (psi)

Most of the references consulted recommend a minimum safety factor of 2.0. The authors are in complete agreement with this recommendation. Thus, if the calculated safety factor is greater than 2.0, the shaft can be considered structurally adequate. If not, design changes need to be instituted to correct the situation.

If the material fatigue properties are not immediately available, Mil. Std. 167 [51] provides a rough rule of thumb for estimating the maximum allowable value of equivalent fully-reversing stress. They recommend that the equivalent stress in steel shafts be kept below 1/25 of the material's ultimate tensile strength. This recommendation, which has an inbuilt safety factor of 2.0, should only be used for ballpark estimates.

Peak Torque

The second criterion to be considered is the peak torque occurring in components such as gears and couplings. The peak torque is simply equal to the sum of the mean transmitted torque and the induced cyclic torque. Most gears and couplings are rated for the maximum continuous torque that they may carry. Although the peak torque in vibration occurs only once in a cycle, it is often taken by the same tooth on at least one of the gears. Such a tooth is, thereby, continuously exposed to this torque. Thus, the authors recommend that the peak torque be kept below the continuous rating for these components.

Torque Reversals

The third and final criterion concerns components that operate with backlash such as gears, splines, and geared couplings. Under normal circumstances, such components are continuously loaded in one direction and the backlash is a total nonfactor. However, if the magnitude of the induced vibratory torque at one of these locations exceeds the average transmitted torque, the applied torque becomes instantaneously negative. This is an indication of a reversal in direction of the applied torque and is known as a torque reversal.

When a torque reversal occurs, the drive surfaces in the gear or spline separate. The negative applied torque causes the teeth to move through their backlash until they make contact on their reverse sides. Once the torque changes sign again, the teeth are driven back through the backlash until they resume contact on their original surfaces.

This phenomenon causes the teeth to continuously pound against each other. This causes shock loading on the teeth which results in loads much greater than the normal design load. This often eventually leads to pitting and wear of the tooth surfaces which is frequently followed by tooth fatigue fracture. Torque reversals, therefore, can have catastrophic consequences.

There are many references that advocate the avoidance of torque reversals at backlash interfaces under all conditions. Although this is a worthy and desirable goal, the authors feel it is overconservative. There is no question that torque reversals cannot be tolerated when the system is operating at anywhere close to its maximum torque. However, at very low transmitted torque levels, the motion through the backlash is less likely to cause problems.

Torque reversals generate problems because the impact loading they produce yields gear loadings that are higher than those designed for. Determination of the amplification of the transmitted load due to impact requires a sophisticated dynamic analysis that is outside the scope of this work. However, Shigley [52] confirms that the universal rule of thumb of doubling the transmitted load to account for impact effects is conservative. Therefore, if a torque reversal occurs when the transmitted torque is below one-half of its maximum value, the resulting gear load would still be below the design load.

Accordingly, torque reversals occurring at these transmitted torque levels may be acceptable. However, it still must be remembered that torque reversals introduce a pounding effect that is absent during normal power transmission. This hammering, even at low force levels, could eventually lead to wear. Thus, in order for a torque reversal situation to be accepted, it must be validated from a tribological standpoint.

Transient Analysis

There are some situations, such as the starting of synchronous motors, where a steady state solution is totally inappropriate. In these cases, a transient analysis must be performed. These analyses

are very different from their steady state counterparts, both in the procedures used and the criteria for acceptability. Some of the major differences between transient and steady state situations are as follows:

• The maximum vibratory torques and stresses in transient problems are often less than the steady state values. This is because they often do not have sufficient time to build up to the steady state values. Chapman [53] provides the following equation for the buildup of torque at resonance with no damping:

$$\tau_{peak} = (N + .5) \bullet \pi \bullet \tau_{exc} \tag{53}$$

where:
τ_{peak} = Peak torque
N = Number of resonant cycles
τ_{exc} = Excitation torque

• In general, transient resonances are not as dangerous as those at steady state. This is due to two factors. The first is the lower induced torque amplitude mentioned above. Additionally, transient resonances exist for only a finite number of cycles. Thus, components need not endure their induced stresses for infinite life.

• In transient cases, there is a lag in the appearance of the peak response. When a system is accelerating, the peak torques will occur at a speed above the resonant speed and during deceleration, the peaks occur at a speed below the critical value. Thus, in both cases, the maximum response does not occur until after the steady state resonant point has been passed through.

• The system's dynamics have a large effect on transient performance. Acceleration and deceleration rates are critical since they determine the dwell time at resonance.

• The uncertainty in magnitude of the various damping factors is less of a concern in transient systems. Steady state problems are extremely sensitive to the assumed values of damping since their resonant dynamic magnifiers are normally extremely high, given the low levels of damping typical for torsional systems. In transient situations, the dynamic magnifiers are usually much lower and the level of sensitivity is correspondingly lower.

• Unlike steady state situations, increased damping is not always beneficial. This is because higher damping values tend to increase the speed range over which the dynamic magnifier is near its maximum value. Thus, a situation can be envisioned in which increasing the system's damping level would increase the dwell time at resonance and the number of fatigue cycles.

Analysis Methods

Since there are many computer programs available for solving transient vibration problems, the discussion of solution procedures will be kept brief. Transient problems are sometimes solved using transform methods. These involve the transfer of information between the time and frequency domains via Laplace or Fourier transforms. These procedures are adequate for completely linear systems but encounter problems when confronted with nonlinearities.

Modal methods, similar to those discussed for steady state problems, are also used on transient problems. These methods suffer from the same problems as the transform methods in that they do not readily handle nonlinearities.

The most robust solution procedures for transient problems are numerical methods. In these, the differential equations of motion for the disks are integrated numerically using methods such as fourth-order Runge-Kutta and the Newmark-ß method. The analysis begins at time zero with all parameters set to their initial values. The numerical approximations, which define a parameter's new value in terms of its previous value, are then used to determine all parameter values after the first time increment. This procedure is continued in a time-marching manner until all transients decay and the system reaches the steady state condition. This procedure, therefore, estimates the time history of all relevant parameters in the system. Evans, et. al. [44], Chen [45], and Szenasi and von Nimitz [54] all discuss numerical integration methods in much greater detail.

It should be noted that several authors comment on the large amount of computer time required to perform transient analysis using numerical integration methods. The user should, therefore, be advised that reduction of the number of elements in the model should be investigated prior to running this type of analysis.

Lewis Procedure

In addition to the rigorous procedures discussed above, Lewis [55] provides a simplified procedure for estimation of the dynamic magnifier for a system accelerating or decelerating at a uniform rate. Although he was working with a single degree of freedom system, his results also provide good estimates for torsional systems with multiple disks. The dynamic magnifier, which Lewis [55] refers to as the resonance factor, for a transient system is defined as follows:

$$DM = \tau_{peak} / \tau_{exc} \tag{54}$$

where:
DM = Dynamic magnifier
τ_{peak} = Peak vibratory torque
τ_{exc} = Excitation torque

A plot of steady state dynamic magnifier *vs* excitation frequency yields the well-known vibration response plot, similar to Figure 2, which has sharp peaks at all of the natural frequencies. When there is no damping in the system, the dynamic magnifier at resonance is theoretically equal to infinity.

As previously pointed out, the dynamic magnifier at resonance for a transient situation is usually somewhat less than the steady state value. Lewis [55] noted that the reduction is strongly dependent on the acceleration or deceleration rate. He presents this relationship as a function of a dimensionless parameter he calls q, which is defined as follows:

$$q = f_n^2 / a \tag{55}$$

where:
q = Acceleration (or deceleration) parameter
f_n = Natural frequency under consideration (Hz)
a = Acceleration (or deceleration) rate (Hz/sec)

The parameter q represents the number of free vibrations that a system would execute between the time when the system is at zero speed and the time when resonance is achieved. In his definition, resonance occurs when the driving frequency is equal to the natural frequency, not at the point of peak response. Thus, q is basically a measure of the relative speed of acceleration or deceleration. Small values of q represent rapid transients while a value of infinity corresponds to the steady state condition. The dynamic magnifier at resonance, thus, increases as q is increased. The lowest value likely to be observed in a practical system is approximately 10.

Lewis [55] presents curves of dynamic magnifier *vs* excitation frequency ratio for various values of q and assorted damping ratios. The maximum transient dynamic magnifier can be obtained from the peak of the appropriate curve. Additionally, Wachel and Szenasi [16] provide a plot of peak dynamic magnifier as a function of q and the steady state resonant dynamic magnifier.

From both of these sources, it can be seen that the difference between the peak transient and steady state dynamic magnifiers is

not very much unless the damping level is very small or the acceleration is extremely rapid. As the system damping is increased, the transient response curves begin to approach the steady state curves. Additionally, it is seen that the dynamic magnifiers for the deceleration cases are slightly higher than the corresponding acceleration values.

Lewis [55] also provides the following equation for the peak dynamic magnifier in a transient, undamped system:

$$DM_{peak} = 3.67 \bullet q^{.5} \pm .354 \qquad (56)$$

The plus sign should be used for decelerations while the minus sign corresponds to the acceleration case.

Analysis Methodology

During the course of a torsional vibration analysis, there are three common situations that require transient analysis, all involving electrical machines. The first case occurs when an AC motor is initially powered. As was mentioned previously, this condition is marked by large motor torque pulsations at line frequency that die out rapidly. If the system has a natural frequency in the vicinity of line frequency, an analysis of this condition must be performed. Pollard [31] provides beneficial information for the analysis of this case. It should be noted that this case need not be analyzed when the motor is started using an active variable frequency drive since the starting pulsations do not occur in this situation. However, as previously noted, this is an anomalous situation since most VFDs are inactive during starting.

The second condition is the shorting of the terminals of an AC motor or generator. For this case, torque pulsations occur at one and two times the electrical supply frequency. Once again, Pollard [31] provides guidelines for the analysis of this situation.

For machines driven by conventional controllers, the short circuit analysis needs to be performed only if the system has natural frequencies near line or twice line frequency. However, the situation for motors driven by variable frequency drives is more complicated. Since the supply frequency to these motors varies, the likelihood for resonance is much greater. Thus, these devices should be analyzed for shorts at all natural frequencies that could potentially be excited.

Synchronous Motor Startups

The above two cases only need to be analyzed in the unfortunate situation where the system has a natural frequency in the vicinity of the excitation frequencies. On the other hand, the third situation, that of the starting of a synchronous motor, must be analyzed for all systems containing these motors and having a natural frequency less than 120 Hz. Again, the exception for when the synchronous motor is started with an LCI should be noted.

The startup of synchronous motors is probably the most significant transient phenomenon that must be dealt with when analyzing torsional systems. As was previously discussed, these devices generate pulsating torques at twice slip frequency during starting. As was shown in the Campbell diagram of Figure 12, these pulsations excite all natural frequencies between zero and 120 Hertz.

The first thing that must be done when analyzing this phenomenon is the obtainment of an accurate torque *vs* speed curve from the motor manufacturer. This curve should include both the average and pulsating torque characteristics over the entire speed range from standstill to synchronous speed. An illustration of a typical torque-speed curve is presented in Figure 11.

Both the average and pulsating torque characteristics play a large role in determining the severity of the vibration during starting. The pulsating torque's role is obvious since it represents the vibratory excitation torque. However, the average torque is also important since it determines the acceleration rate of the drive train.

During starting, the net torque available to accelerate the system is equal to the motor's average torque minus the load torque. It is, therefore, helpful to also have the load's torque *vs* speed curve, although many common load torques can be approximated as being proportional to the square of the speed. The system's acceleration rate in the vicinity of the critical speed is crucial because it determines the length of time and number of cycles that the machine spends at resonance.

To estimate the time spent at resonance, Brown [56] recommends the definition of a resonant speed band centered about the critical speed. Chen, McLaughlin, and Malanoski [46] point out that this band should be relatively small since torsional systems are usually lightly damped and, thus, have narrow resonant peaks. The time spent within this band is critical for two reasons. The first is that long resonance times give the vibration amplitude a chance to build up to the steady state value. Additionally, the number of damaging fatigue cycles experienced is directly proportional to the resonance dwell time.

Synchronous motor startups are usually analyzed using a numerical integration time-marching scheme. While these provide an accurate time history for every element in the system, they are usually costly and time-consuming. As an alternative, Chen, McLaughlin, and Malanoski [46] offer a simple method for estimating the maximum cyclic torques and stresses that occur at resonance with the fundamental frequency. The method is modal in nature and only requires the motor's torque-speed curve and the fundamental mode shape for implementation. With this information, the calculation can be performed in a matter of minutes.

The potential shortcomings of this method are that it only deals with resonances with the fundamental mode and does not attempt to determine the number of cycles spent at the maximum stress level. The first item may not be as large of a problem as it may appear since Pollard [31], Wright [47], and Sohre [57] all claim that synchronous motor resonance problems usually occur at the fundamental frequency. There are several reasons for this. First of all, the fundamental frequency is often characterized by large displacement at the motor so it is especially vulnerable to motor torque variations. Secondly, the fundamental mode is always the mode having the highest energy level. Finally, the resonance with the fundamental occurs at the highest speed due to the inverse slope of the motor's excitation line so the pulsating torque there is likely to be higher than for other modes.

The second criticism can be dealt with by making a conservative estimate of the number of cycles at maximum stress. As Chen, et al. [46], point out, the resonance band is usually narrow enough that the acceleration rate can be taken as constant. This rate can be estimated by the following equation:

$$\alpha = (\tau_{ave} - \tau_{load}) / J_{tot} \qquad (57)$$

where:

α = Acceleration rate through resonance (rad/sec^2)
τ_{ave} = Average motor torque at resonant speed (in−lbf)
τ_{load} = Load torque at resonant speed (in−lbf)
J_{tot} = Total system inertia (in−lbf−sec^2)

The time spent at resonance can then be determined by dividing the width of the resonance band by the acceleration rate. The number of cycles at maximum stress can then be obtained by multiplying the vibratory frequency by the time spent at resonance to obtain the number of resonant cycles and assuming that these cycles are all at maximum stress. To provide a point of reference, Sohre [57] claims that a typical startup contributes between 10 and 20 high stress cycles.

Of course, use of this method must be tempered by judgment. There are some situations in which the fundamental mode may not be the most dangerous. For instance, this method would not be

appropriate for a system having a fundamental mode shape with little activity at the motor. However, in situations where it can be used, this procedure represents a large time and labor saver.

Analysis Results

Regardless of the condition analyzed and the analysis method utilized, the primary objective of a transient analysis is to determine the maximum cyclic torques and stresses induced in the various model elements. Although the goal is the same as for steady state analysis, the acceptance criteria are significantly different.

First of all, the stress levels are not compared to the endurance limit since the number of cycles at maximum stress is much lower than for a steady state resonance. Furthermore, there is often more than one stress condition that must be considered for each shaft since the induced stress verses time profile often looks like that of Figure 21.

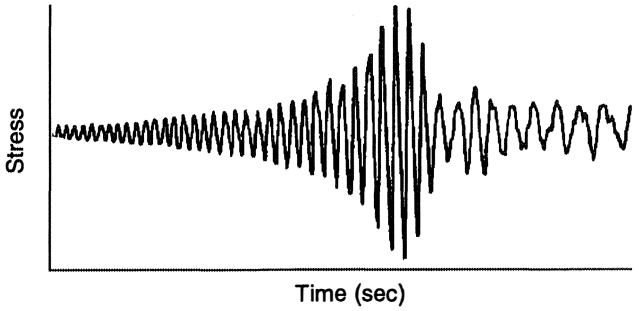

Figure 21. Typical Transient Response.

Determination of structural adequacy is easiest for the short circuit condition. Since a given machine can be expected to experience, at most, a few short circuits during its lifetime, fatigue is not a concern. Accordingly, the maximum induced stresses should be compared directly to the material's yield and ultimate strengths in shear.

For the other two cases, adequacy should be determined by first calculating the equivalent fully-reversing stress for each induced cyclic stress using the same procedure used for steady state stresses. Secondly, the number of cycles at each stress condition should be determined by multiplying the number of stress cycles per start by the expected number of starts in the lifetime of the drive train. The allowable number of cycles for each stress state should then be found from an S-N curve for the material. The actual number and allowable number of cycles should then be used in a cumulative damage algorithm, such as a Miner's summation, to determine structural adequacy.

In addition to the above check for fatigue, the maximum stress also should be compared to the shaft's shear yield strength (or ultimate strength if yielding is permissible) to assure that a one-shot failure does not occur. In the same vein, the maximum torques should be compared to the maximum torque ratings for gears, splines, and couplings.

In contrast to the steady state situation, torque reversals at components with backlash are not cause for panic in the transient situation. The greatly reduced number of reversal cycles in the transient case makes tooth pitting and wear a much smaller concern. Szenasi and von Nimitz [54] note that transient reversals are very common and are often allowed for in the design of gears and geared couplings.

Synchronous Motor Characteristics

If the analysis reveals that the system has a transient stress problem, the designer has several options for rectification. Any of the generic solutions to interference problems to be discussed in a later section can be implemented. Additionally, synchronous motors have some unique characteristics that can also provide solutions. Some of these traits are as follows:

- There is always a point in the speed range where the motor's direct and quadrature axis torques cross, as is seen from Figure 11. Since the pulsating torque is proportional to the difference between these two numbers, there is no pulsating torque at the crossover speed. Thus, if the system can be altered to place the resonant point close to the crossover point, substantial benefit would result. This can be accomplished either by changing the system to alter the natural frequency or by moving the crossover point by changing the motor's design.

- Since both the motor and load average torque-speed curves often contain peculiarities, the net accelerating torque is far from constant over the speed range. The accelerating torque should be plotted as a function of speed and changes should be enacted to locate the problem resonant point at a speed where the accelerating torque is high to minimize resonance dwell time.

- In general, reduction of the pulsating torque is beneficial. The pulsating torque at a given speed can be easily reduced by altering the motor's design or by adding a resistance in series with the motor. The resistance acts to reduce the voltage across the motor's terminals which reduces the pulsating torque since it is approximately proportional to the square of this voltage. However, this change is a double-edged sword since the ratio of pulsating torque to average torque is approximately constant. The average torque will, therefore, be reduced by about the same amount. However, there are some cases, such as when the yield strength or ultimate strength is exceeded, where the net effect is positive.

- In contrast to the above item, there are situations where an increase in average torque is beneficial, in spite of the corresponding rise in pulsating torque. An example is a system with a relatively large load torque. In such a system, a small increase in average torque could result in a much faster acceleration rate and improved performance.

- In general, solid pole motors generate more problems during starting than do those having laminated rotors. Thus, the simple change from a device with solid poles to one with laminated poles could eliminate an overloading problem. However, a switch to the more costly laminated design must be justified from an economic standpoint.

- Synchronous motors often have a dip in their average torque curve at about one-half of synchronous speed. Since the pulsating torque characteristic usually does not contain this dip, resonances close to this speed are usually troublesome and should be avoided.

ELIMINATION OF INTERFERENCE PROBLEMS

If the previous analysis reveals that there are any interference points that constitute a problem from a stress or gear unloading standpoint, the user generally has four options for rectification. First of all, the interference point can be eliminated by altering the cognizant natural frequency or, less likely, changing the excitation frequency. Secondly, the user can make design changes to reduce the excitation applied to the system. Thirdly, the user can add damping to the system to attenuate the resonant response. Lastly, the user can designate a barred speed range centered about the interference point in which the machine is forbidden from operating continuously.

Alteration of Natural Frequencies

The option that should be investigated first is removal of the problem interference point via change of the natural frequency.

Natural frequencies may be altered by either changing disk inertias or shaft stiffnesses. Increasing spring rates tends to raise natural frequencies while increasing inertias has the opposite effect.

In order to identify candidate elements for modification, the appropriate mode shape should be reviewed. In general, shaft elements that experience significant twisting in that mode are candidates for change. This is because the sensitivity of a natural frequency to a change in a particular shaft element is proportional to the total strain energy stored in that shaft. Since strain energy is proportional to the square of the angle of twist, altering an element experiencing considerable twisting will have a large impact on the natural frequency. On the other hand, shafts having very little twisting can be altered by an order of magnitude and still have a negligible effect on the natural frequency.

In turbomachinery, couplings are usually the easiest components to change. Therefore, the twist occurring in them should be examined closely to determine if there is any potential benefit to their alteration. Fortunately, the fundamental mode in many turbomachinery drives is characterized by twisting exclusively in one coupling. This occurs because systems often contain a coupling whose stiffness is an order of magnitude lower than any other shaft in the system. Since most vibration problems occur with the fundamental mode, a simple coupling change is often sufficient to solve the problem.

Although impellers are usually not as easily altered as couplings, their modification can also eliminate a problem interference. As is the case with shaft elements, the mode shape provides a good indication of which impellers should be altered. The sensitivity of a natural frequency to change of a specific inertia is proportional to the percentage of the system's kinetic energy stored in that disk. Since the energy is proportional to the square of the maximum amplitude, only disks having significant vibratory amplitudes should be considered for modification.

If a shaft element or inertia change is found to be sufficient to move the problem interference point away from the operating range with sufficient margin, that particular point can be dismissed. However, any change to the system can alter all natural frequencies, not just the one being considered. The new natural frequencies must, therefore, be calculated and checked for any new interferences that may have been generated.

Another way to eliminate a problem interference point is by placement of a hydraulic coupling between the excitation source and region where shaft overstressing or gear unloading is taking place. As stated previously, hydraulic couplings serve to divide the assembly into two independent systems, thus, isolating the two systems from each other. For instance, if torque pulsations from a synchronous motor were producing high stresses in a shaft remote from the motor, a fluid coupling placed at the motor's output shaft would remove the problem. Of course, if this tactic is used, the two new resulting systems would need to be freshly analyzed.

A less common method of eliminating interferences is via changing the order number of the exciting component. This option is only viable for order numbers above two since the 1× and 2× excitations are always assumed to be present. However, if the excitation is caused by the blade pass frequency of an impeller or a gear meshing frequency, it can be altered by merely changing the number of blades or gear teeth, as long as the change does not adversely impact performance.

The second alternative for escaping trouble is reduction of the excitation driving the system. The applicability of this method is dependent on the nature of the exciting mechanism. If the excitation arises from an electric motor or generator, design changes can often be made which reduce the torque fluctuations. Additionally, excitations generated by gears, particularly displacement excitations, can be reduced by applying tighter tolerances to the gear tooth profile.

The third option is addition of damping to the system. There are many types of couplings available that produce significant damping via elastomers or oils contained within. Additionally, even if the excitation source and critically stressed shaft are located such that introduction of a hydraulic coupling would not isolate them from each other, such a coupling can introduce substantial damping to the assembly. Finally, there are many devices such as Lanchester dampers, whose sole purpose is to provide torsional damping, that can be utilized.

Regardless of the damping element chosen, it should be strategically located in order to be effective. As was discussed previously, dampers are only effective if they are located in regions of significant vibration activity for the mode under consideration. The appropriate mode shape, therefore, should be utilized to determine optimum locations for dampers. Ideally, dampers should be positioned in places where the mode shape reveals the absolute or relative displacement to be near maximum.

The final option is designation of a certain speed range to be off-limits for steady operation. The desirability of this option is dependent on the level of hardship it imposes on the user. In general, this option is used only in cases where none of the other alternatives can be practically implemented.

OVERALL ANALYSIS PROCEDURE

At this point all of the component steps of a torsional vibration analysis procedure have been described in detail. To summarize, a chronological listing of these steps is as follows:

1. Generate lumped parameter model.
2. Determine undamped natural frequencies and mode shapes.
3. Verify undamped analysis results using hand calculations.
4. Generate Campbell diagram.
   - Plot natural frequencies.
   - Plot operating speed range.
   - Plot excitation lines (See Table 1 for guidelines).
5. Determine all interference points from Campbell diagram.
   - All intersection points within operating speed range
   - All intersection points outside of speed range that don't have adequate margin (see Equation (22)).
   - For systems containing AC machines, natural frequencies at line and/or twice line frequency
   - All intersection points with synchronous motor twice slip frequency excitation line
   - All intersection points with active VFD excitation lines
6. Use inspection techniques to eliminate interference points.
   - Points excited by torques located near nodes
   - Points excited by gear displacements located away from nodes
   - Points that are obviously less severe than other interference points involving same mode
   - Points where mode shapes show little twist in vulnerable regions
7. Determine excitation torque magnitudes.
   - Generic 1× excitations
   - Generic 2× excitations
   - Gear excitations
   - Impeller excitations
   - Propeller excitations
   - AC machine excitations
     - Steady state torques
     - Peak torques during short circuits
     - Peak torques during initial powering
   - Variable frequency drive excitations
8. Perform preliminary steady state forced vibration analysis.
   - Identify interference points that must be analyzed (all except for those listed under transient analysis).

- For each cognizant interference point, execute the following steps:
  - Apply excitation at appropriate location.
  - Apply damping of one percent of critical to all shaft elements.
  - Determine induced torques and stresses throughout system.
  - Evaluate results:
    - All shafts must have infinite lives.
    - Peak torques in gears, splines, and couplings must not exceed their continuous ratings.
    - Effects of torque reversals in connections having backlash must be evaluated.
  - If results indicate a potential problem, proceed to step 9.

9. Perform rigorous steady state forced vibration analysis.
   - Determine damping coefficients for system components.
     - Loads (impellers, propellers, generators, etc.)
     - Drivers (motors, turbines, etc.)
     - Windage
     - Fluid-film journal bearings
     - Couplings (elastomeric, hydraulic, etc.)
     - Cyclic speed variation
   - For each cognizant interference point, execute the following steps:
     - Apply excitations and damping at appropriate locations.
     - Apply damping of one percent of critical to all shaft elements.
     - Determine induced torques and stresses throughout system.
     - Evaluate results (see step 8).
     - If results indicate a potential problem, proceed to step 12.
10. Perform preliminary transient forced vibration analysis.
    - Identify interference points that must be analyzed (see Table 4).
    - For each cognizant interference point, execute the following steps:
      - Apply excitation at appropriate location.
      - Apply damping of one percent of critical to all shaft elements.
      - Determine induced torques and stresses in system as function of time.
      - Evaluate results.
        - Fatigue lives of all shafts must be satisfactory.
        - Peak torques in gears, splines, and couplings must not exceed their maximum ratings.
      - If results indicate a potential problem, proceed to step 11.
11. Perform rigorous transient forced vibration analysis.
    - Determine damping coefficients for system components (see step 9).
    - For each cognizant interference point, execute the following steps:
      - Apply excitations and damping at appropriate locations.
      - Apply damping of one percent of critical to all shaft elements.
      - Determine induced torques and stresses in system as function of time.
      - Evaluate results (see step 10).
      - If results indicate a potential problem, proceed to step 12.
12. Implement modifications to eliminate interference problems.
    - Investigate means of changing natural frequencies.
    - Investigate methods of changing excitation frequencies.
    - Investigate means of reducing excitation magnitudes.
    - Investigate feasibility of adding damping to system.
    - If necessary, designate speed range to be off-limits (usually last resort).
13. Analyze new system resulting from step 12 changes.

It is seen that steps one through five involve the identification of all of the machine's interference points. The remaining steps are then utilized to dismiss points, one by one, until there are none remaining. When this point is reached, the system is viable.

CONCLUSIONS

A comprehensive procedure for the analysis of torsional vibration has been presented. The methodology is general enough that it should be applicable to any turbomachinery configuration that may be encountered. The key points that should be emphasized are as follows:

- A thorough torsional vibration analysis should always be included as an integral part of the turbomachinery design process.
- The essence of torsional vibration analysis is identification of all resonance points and determination of the system's ability to withstand them.
- A Campbell diagram should be generated as soon as possible to provide visibility into the overall situation.
- Systems employing synchronous motors and/or variable frequency drives should be treated with extra caution.
- Manufacturers of equipment such as motors and couplings should be consulted with regards to the torsional vibration characteristics of their products.
- The presence of resonance points in a system is not an automatic harbinger of disaster. Many resonant points can be shown to be harmless via various methods.
- Torsional vibration analysis is not an exact science. Although many of the calculation procedures are relatively sophisticated, the role of the skill and judgment of the analyst should not be underestimated.

REFERENCES

1. Vance, J. M., *Rotordynamics of Turbomachinery,* New York, New York: John Wiley and Sons (1988).
2. Ker Wilson, W., *Practical Solution of Torsional Vibration Problems, Volumes 1, 2, and 3,* New York, New York: John Wiley and Sons, 3rd Ed. (1956).
3. Eshleman, R. L., "Torsional Response of Internal Combustion Engines," ASME Journal of Engineering for Industry, pp. 441-449 (May 1974).
4. Bisshopp, K. E., "Forced Torsional Vibration of Systems with Distributed Mass and Internal and External Damping," ASME Journal of Applied Mechanics, pp. 8-12 (March 1959).
5. Triezenberg, D. M., "Characteristic Frequencies and Mode Shapes for Turbogenerator Shaft Torsional Vibrations," IEEE Transactions on Power Apparatus and Systems, pp. 352-357 (January/February 1980).
6. Simmons, H. R. and Smalley, A. J., "Lateral Gear Shaft Dynamics Control Torsional Stresses in Turbine-Driven Compressor Train," ASME Journal of Engineering for Gas Turbines and Power, pp. 946-951 (October 1984).
7. Lund, J. W., "Critical Speeds, Stability and Response of a Geared Train of Rotors," ASME Journal of Mechanical Design, pp. 535-539 (July 1978).
8. Nestorides, E., A., *Handbook on Torsional Vibration,* London: Cambridge University Press (1958).
9. O'Connor, B. E., "The Viscous Torsional Vibration Damper," SAE Quarterly Transactions, pp. 87-97 (January 1947).
10. Den Hartog, J. P. and Ormondroyd, J., "Torsional-Vibration Dampers," ASME Transactions, paper APM-52-13 (1930).
11. Brown, R. N., "Torsional Damping–Transient and Steady State," *Proceedings of the Thirteenth Turbomachinery*

Symposium, Turbomachinery Laboratory, Texas A&M University, College Station, Texas (1984).

12. McCann, G. D. and Bennett, R. R., "Vibration of Multifrequency Systems During Acceleration Through Critical Speeds," ASME Journal of Applied Mechanics, pp. 375-382 (December 1949).
13. Pollard, E. I., "Transient Torsional Vibration Due to Suddenly Applied Torque," ASME Journal of Engineering for Industry, pp. 595-602 (May 1972).
14. Simmons, H. R. and Smalley, A. J., "Effective Tools for Diagnosing Elusive Turbomachinery Dynamics Problems in the Field," ASME Journal of Engineering for Gas Turbines and Power, pp. 470-477 (October 1990).
15. Hershkowitz, H., "Torsional Vibration Measurement in Preventive Maintenance of Rotating Machinery," Scientific-Atlanta, Inc., Randolph Township, New Jersey.
16. Wachel, J. C. and Szenasi, F. R., "Analysis of Torsional Vibrations in Rotating Machinery," *Proceedings of the Twenty-Second Turbomachinery Symposium,* Turbomachinery Laboratory, Texas A&M University, College Station, Texas (1993).
17. Hammons, T. J., "Electrical Damping and its Effect on Accumulative Fatigue Life Expenditure of Turbine-Generator Shafts Following Worst-Case Supply System Disturbances," IEEE Transactions on Power Apparatus and Systems, pp. 1552-1565 (June 1983).
18. "Reader's Guide to Subsynchronous Resonance," IEEE Transactions on Power Systems, pp. 150-156 (February 1992).
19. Rana, R. D. and Schulz, R. P., "Generator Loss of Field: Experience and Studies for AEP's Rockport Plant," Proceedings of the American Power Conference.
20. Joyce, J. S., Kulig, T., and Lambrecht, D., "Torsional Fatigue of Turbine-Generator Shafts Caused by Different Electrical System Faults and Switching Operations," IEEE PES Winter Meeting, New York, New York (1978).
21. Undrill, J. M. and Hannett, L. N., "Turbine-Generator Impact Torques in Routine and Fault Operations," IEEE PES Winter Meeting, New York, New York (1978).
22. Andriola, A. D., "Torsional Vibration in Geared-Turbine Marine Propulsion Plants–An Introduction to the Subject," Transactions of the Society of Naval Architects and Marine Engineers, pp. 733-752 (1950).
23. Den Hartog, J. P., *Mechanical Vibrations,* Fourth Edition, New York, New York: McGraw-Hill Book Company (1956).
24. Schlegel, R. G., King, R. J., and Mull, H. R., "How to Reduce Gear Noise," Machine Design, pp. 134-142 (February 1964).
25. Mayer, C. B., "Torsional Vibration Problems and Analysis of Cement Industry Drives," IEEE Transactions on Industry Applications, pp. 81-89 (January/February 1981).
26. Ehrich, F. F., *Handbook of Rotordynamics,* New York, New York: McGraw-Hill Inc. (1992).
27. Poritsky, H., "Torsional Vibration in Geared Turbine Propulsion Equipment," ASME Journal of Applied Mechanics, pp. A-117 - A-124 (September 1940).
28. "Torsional Vibrations," 1988 Seminar on Vibration Analysis and Diagnostic Techniques for Rotating Machinery, Mechanical Technology Incorporated, Latham, New York (September 1988).
29. Artilles, A., Smalley, A. J., and Lewis, P., "Mill Drive System Vibrations," Proceedings of the National Conference on Power Transmission, Chicago, Illinois (October 1975).
30. Yates, H. G., "Prediction and Measurement of Vibration in Marine Geared-Shaft Systems," Proceedings of the Institution of Mechanical Engineers, pp. 611-642 (1955).
31. Pollard, E. I., "Synchronous Motors ... Avoid Torsional Vibration Problems," Hydrocarbon Processing (February 1980).
32. Wolff, F. H. and Molnar, A. J., "Variable-Frequency Drives Multiply Torsional Vibration Problems," Power, pp. 83-85 (June 1985).
33. Grgic, A., Heil, W., and Prenner, H., "Large Converter-Fed Adjustable Speed AC Drives for Turbomachines," *Proceedings of the Twenty-First Turbomachinery Symposium,* Turbomachinery Laboratory, Texas A&M University, College Station, Texas (1992).
34. Murphy, S. P., "Application of Variable Speed Electric Motors for Pumps," *Proceedings of the Tenth International Pump Users Symposium,* Turbomachinery Laboratory, Texas A&M University, College Station, Texas (1993).
35. Sheppard, D. J., "Torsional Vibration Resulting from Adjustable Frequency AC Drives," IEEE Transactions on Industry Applications, pp. 812-817 (September/October 1988).
36. Hudson, J. H., "Lateral Vibration Created by Torsional Coupling of a Centrifugal Compressor System Driven by a Current Source Drive for a Variable Speed Induction Motor," *Proceedings of the Twenty-First Turbomachinery Symposium,* Turbomachinery Laboratory, Texas A&M University, College Station, Texas (1992).
37. Smalley, A. J., "Torsional System Damping," Proceedings of the 1983 Vibration Institute Seventh Annual Meeting, Houston, Texas (1983).
38. Draminsky, P., "Crankshaft Damping," Proceedings of the Institution of Mechanical Engineers, pp. 416-432 (1948).
39. Shannon, J. F., "Damping Influences in Torsional Oscillation," Proceedings of the Institution of Mechanical Engineers, pp. 387-435 (1935).
40. Dorey, S. F., "Elastic Hysteresis in Crankshaft Steels," Proceedings of the Institution of Mechanical Engineers, pp. 479-510 (1932).
41. Rieger, N. F., "The Role Gears Play in Drive-Train Vibrations," Machine Design, pp. 115-119 (July 1969).
42. Frei, A, Grgic, A., Heil, W., and Luzi, A., "Design of Pump Shaft Trains Having Variable-Speed Electric Motors," *Proceedings of the Third International Pump Symposium,* Turbomachinery Laboratory, Texas A&M University, College Station, Texas (1986).
43. Thames, P. B. and Heard, T. C., "Torsional Vibrations in Synchronous Motor-Geared-Compressor Drives," AIEE Transactions, pp. 1053-1056 (December 1959).
44. Evans, B. F., Smalley, A. J., and Simmons, H. R., "Startup of Synchronous Motor Drive Trains: The Application of Transient Torsional Analysis to Cumulative Fatigue Assessment," ASME paper 85-DET-122 (1985).
45. Chen, W. J., "Torsional Vibrations of Synchronous Motor Driven Trains Using p-Method," ASME Journal of Vibration and Acoustics, pp. 152-160 (January 1995).

46. Chen, H. M., McLaughlin, D. W., and Malanoski, S. B., "A Generalized and Simplified Transient Torque Analysis for Synchronous Motor Drive Trains," *Proceedings of the Twelfth Turbomachinery Symposium,* Turbomachinery Laboratory, Texas A&M University, College Station, Texas (1983).

47. Wright, J., "Large Synchronous Motor Drives: A Review of the Torsional Vibration Problem and its Solution," Koppers Company, Inc.

48. Tuplin, W. A., *Torsional Vibration,* New York, New York: John Wiley and Sons (1934).

49. Den Hartog, J. P. and Li, J. P., "Forced Torsional Vibrations with Damping: An Extension of Holzer's Method," ASME Journal of Applied Mechanics, pp. A-276-A-280 (December 1946).

50. Badgley, R. H. and Laskin, I., "Program for Helicopter Gearbox Noise Prediction and Reduction," MTI USAAVLABS Technical Report 70-12, Ft. Eustis, Virginia (March 1970).

51. MIL STD 167, Mechanical Vibrations of Shipboard Equipment (Reciprocating Machinery and Propulsion System and Shafting) (1974).

52. Shigley, J. E., *Mechanical Engineering Design,* Third Edition, New York, New York: McGraw-Hill Book Company (1977).

53. Chapman, C. W., "Zero (or Low) Torsional Stiffness Couplings," Journal of Mechanical Engineering Science, *11,* (1), pp. 76-87 (1969).

54. Szenasi, F. R. and von Nimitz, W. W., "Transient Analysis of Synchronous Motor Trains," *Proceedings of the Seventh Turbomachinery Symposium,* Turbomachinery Laboratory, Texas A&M University, College Station, Texas (1978).

55. Lewis F. M., "Vibration During Acceleration Through a Critical Speed," ASME Transactions–Applied Mechanics, pp 253-261 (1932).

56. Brown, R. N., "A Torsional Vibration Problem as Associated with Synchronous Motor Driven Machines," ASME Journal of Engineering for Power, pp. 215-220 (July 1960).

57. Sohre, J. S., "Transient Torsional Criticals of Synchronous Motor Driven, High-Speed Compressor Units," ASME Paper 65-FE-22 (1965).

BIBLIOGRAPHY

Alison, N. L., "Hydraulic Couplings for Internal Combustion Engine Applications," ASME Transactions, pp. 81-90 (February 1941).

Badgley, R. H., "Mechanical Aspects of Gear-Induced Noise in Complete Power Train Systems," ASME Paper 70-WA/DGP-1 (1970).

Bigret, R., Coetzee, C. J., Levy, D. C., and Harley, R. G., "Measuring the Torsional Modal Frequencies of a 900 MW Turbogenerator," IEEE Transactions on Energy Conversion, pp. 99-107 (December 1986).

Braund, D. F., "Torsional Vibration," Proceedings of the Institution of Mechanical Engineers, pp. 63-72 (1958).

Costello, M. J., "Understanding the Vibration Forces in Induction Motors," *Proceedings of the Nineteenth Turbomachinery Symposium,* Turbomachinery Laboratory, Texas A&M University, College Station, Texas (1990).

Cox, C. R., "Design Considerations for Acceptable Cabin Noise Levels in Light Helicopters," American Helicopter Society Preprint No. SW-70-23 (1970).

Cudworth, C. J., Smith, J. R., and Mykura, J. F., "Mechanical Damping of Torsional Vibrations in Turbogenerators Due to Network Disturbances," Proceedings of the Third International Conference on Vibrations in Rotating Machinery, Institution of Mechanical Engineers, pp. 139-144 (September 1984).

Cudworth, C. J. and Smith, J. R., "Turbine-generator Shaft Torsional Oscillations Produced by Imbalanced Transmission Network Disturbances," Proceedings of First Parsons International Turbine Conference, Institution of Mechanical Engineers, pp. 241-246 (June 1984).

Doughty, S., "A Rayleigh-Type Inclusion of Shaft Inertia in Torsional Vibration Analysis," ASME Journal of Engineering for Gas Turbines and Power, pp. 831-837 (October 1994).

Eshleman, R. L., "Torsional Vibration of Machine Systems," *Proceedings of the Sixth Turbomachinery Symposium,* Turbomachinery Laboratory, Texas A&M University, College Station, Texas (1977).

Godwin, G. L. and Merrill, E. F., "Oscillatory Torques During Synchronous Motor Starting," IEEE Transactions on Industry and General Applications, pp. 258-265 (May/June 1970).

Graybeal, T. D., "The Nature of Vibration in Electric Machinery," Electrical Engineering, pp. 712-718 (October 1944).

Harris, S. L., "Dynamic Loads on the Teeth of Spur Gears," Proceedings of the Institution of Mechanical Engineers, pp. 87-100 (1958).

Hyde, R. L. and Brinner, T. R., "Starting Characteristics of Electric Submergible Oil Well Pumps," IEEE Transactions on Industry Applications, pp. 133-144 (January/February 1986).

Johnson, D. C., "The Excitation of Resonant Vibration by Gear Tooth Meshing Effects," Proceedings of the International Conference on Gearing, Institution of Mechanical Engineers, London, pp. 18-23 (September 1958).

Kashay, A. M., Voelker, F. C., and Smalley, A. J., "Dynamic Shock Phenomena in Rolling Mills," ASME Journal of Engineering for Industry, pp. 647-659 (May 1972).

Kenney, C. S. and Shih, S., "Prediction and Control of Heavy Duty Powertrain Torsional Vibration," SAE Transactions, pp. 805-814 (1992).

Kimball, A. L. and Lovell, D. E., "Internal Friction in Solids," ASME Transactions, pp. 479-500 (1926).

Lack, A. and Jahnke, C. B., "Torsional Vibrations and Critical Speeds of Shafts," ASME Transactions, pp. 493-523 (1925).

Lambrecht, D. and Kulig, T., "Torsional Performance of Turbine Generator Shafts Especially Under Resonant Excitation," IEEE Transactions on Power Apparatus and Systems, pp. 3689-3702 (October 1982).

Lazan, B. J., "Effect of Damping Constants and Stress Distribution on the Resonance Response of Members," ASME Journal of Applied Mechanics, pp. 201-209 (June 1953)

Lazan, B. J., "Energy Dissipation Mechanisms in Structures, with Particular Reference to Material Damping," Proceedings of Colloquium on Structural Damping, ASME, Atlantic City, New Jersey, pp. 1-34 (December 1959).

Lees, A. W., "Dynamic Loads in Gear Teeth," Proceedings of the Third International Conference on Vibrations in Rotating Machinery, Institution of Mechanical Engineers, pp. 73-79 (September 1984).

Lees, A. W. and Haines, K. A., "Torsional Vibrations of a Boiler Feed Pump," ASME Journal of Mechanical Design, pp. 637-643 (October 1978).

Lewis, F. M., "The Critical Speeds of Torsional Vibration," SAE Journal, pp. 418-431 (November 1920).

Lewis, F. M., "Torsional Vibration in the Diesel Engine," Transactions of the Society of Naval Architects and Marine Engineers, pp. 109-140 (1925).

Mahalingham, S. and Bishop, R. E., "Dynamic Loading of Gear Teeth," Journal of Sound and Vibration, pp. 179-189 (1974).

Mark, W. D., "Analysis of the Vibratory Excitation of Gear Systems: Basic Theory," Journal of the Accoustic Society of America, pp. 1409-1430 (May 1978).

Mayer, C. B., "Torsional Dynamics–An Important Consideration in Large Refiner Drive Systems," 1985 TAPPI Engineering Conference, pp. 105-115 (1985).

Mitchell, R. W., "The Design Office Problem in the Estimation of the Torsional Resonance Characteristics of Small Marine Diesel-Propulsion Units," Proceedings of the Institution of Mechanical Engineers, pp. 133-142 (1943).

Mondy, R. E. and Mirro, J., "The Calculation and Verification of Torsional Natural Frequencies for Turbomachinery Equipment Strings," *Proceedings of the Eleventh Turbomachinery Symposium,* Turbomachinery Laboratory, Texas A&M University, College Station, Texas (1982).

Mruk, G. K., "Compressor Response to Synchronous Motor Startup," *Proceedings of the Seventh Turbomachinery Symposium,* Turbomachinery Laboratory, Texas A&M University, College Station, Texas (1978).

Pollard, E. I., "Torsional Response of Systems," ASME Journal of Engineering for Power, pp. 316-324 (July 1967).

Porter, F. P., "Practical Determination of Torsional Vibration in an Engine Installation which may be Simplified to a Two-Mass System," ASME Transactions–Applied Mechanics, pp. 25-61.

Porter, F. P., "The Range and Severity of Torsional Vibration in Diesel Engines," ASME Transactions–Applied Mechanics, pp. 25-61 (1927).

Reswick, J. B., "Dynamic Loads on Spur and Helical Gear Teeth," ASME Transactions, pp. 635-644 (July 1955).

Rowett, F. E., "Elastic Hysteresis in Steel," Proceedings of the Royal Society, pp. 528-543 (1914).

Schlegel, R. G. and Mard, K. C., "Transmission Noise Control–Approaches in Helicopter Design," ASME Paper 67-DE-58 (1967).

Seireg, A. and Houser, D. R., "Evaluation of Dynamic Factors for Spur and Helical Gears," ASME Journal of Engineering for Industry, pp. 504-515 (May 1970).

Shadley, J. R., Wilson, B. L., and Dorney, M. S., "Unstable Self-Excitation of Torsional Vibration in AC Induction Motor Driven Rotational Systems," ASME Journal of Vibration and Acoustics, pp. 226-231 (April 1992).

Smalley, A. J., "Transient Torsional Vibration," Mechanical Technology Incorporated, Latham, New York (September 1974).

Smith, J. R., Mykura, J. F., and Cudworth, C. J., "The Effect of Hysteretic Damping on Turbogenerator Shaft Torsional Oscillations," IEEE Transactions on Energy Conversion, pp. 152-157 (March 1986).

Spaetgens, T. W., "Holzer Method for Forced-Damped Torsional Vibrations," ASME Journal of Applied Mechanics, pp. 59-63 (March 1950).

Thomsen, W. T., *Theory of Vibration with Applications,* Englewood Cliffs, New Jersey: Prentice Hall, 3rd Ed. (1988).

Tuplin, W. A., "Dynamic Loads on Gear Teeth," Proceedings of the International Conference on Gearing, Institution of Mechanical Engineers, London, pp. 31-42 (September 1958).

Wachel, J. C., "Design Audits," *Proceedings of the Fifteenth Turbomachinery Symposium,* Turbomachinery Laboratory, Texas A&M University, College Station, Texas (1986).

Wachel, J. C., Atkins, K. E., and Tison, J. D., "Improved Reliability through the Use of Design Audits," *Proceedings of the Twenty-Fourth Turbomachinery Symposium,* Turbomachinery Laboratory, Texas A&M University, College Station, Texas (1995).

Wahl, A. M. and Kilgore, L. A., "Transient Starting Torques in Induction Motors," Electrical Engineering–Transactions, pp. 603-607 (November 1940).

Wahl, A. M., "Transient Torques in Induction Motor Drives," ASME Journal of Applied Mechanics, pp. A-17 - A-21 (March 1941).

Walker, D. N., Bowler, C. E., Jackson, R. L., and Hodges, D. A., "Results of Subsynchronous Resonance Test at Mohave," IEEE Transactions on Power Apparatus and Systems, pp. 1878-1889 (September/October 1975).

Walker, D. N., Adams, S. L., and Placek, R. J., "Torsional Vibration and Fatigue of Turbine-Generator Shafts," IEEE Transactions on Power Apparatus and Systems, pp. 4373-4380 (November 1981).

Wang, C. C., "Rotational Vibration with Backlash: Part 1," ASME Paper 77-DET-105 (1977).

Wang, S. M. and Morse, I. E., "Torsional Response of a Gear Train System," ASME Journal of Engineering for Industry, pp. 583-594 (May 1972).

Williams, P. N., McQuin, N. P., and Buckland, J. E., "The Importance of Complete Drive Train Analysis for Brushless Salient Pole Motor Drives," Fourth International Conference on Electrical Machines and Drives, IEE-England, pp. 210-214 (1989).

ACKNOWLEDGMENTS

The authors would like to recognize and thank their colleagues at MTI who assisted in the generation of this presentation. Specifically, publication of this tutorial would not have been possible without the contributions and talents of Mike Cronin, Sandy MacCue, Donna Rivers, and Shirl Smith.